[RI3]

Variational approach to optical flow estimation managing discontinuities

Paolo Nesi

Projection of the 3D velocity of real objects on the image plane is often called the 'velocity field'. The estimation of this field is one of the most important research topics in computer vision. In the literature, there are numerous solutions which adopt a sort of continuity equation called optical flow constrain (OFC). The solution of this constraint equation is usually called the 'optical flow' field, and can be considered equal to the velocity field under particular assumptions. The structure of the OFC equation makes the optical flow estimation an ill-posed problem, like many other inverse problems in early-vision. For this reason, many reglarization techniques were used in the past for estimating optical flow. The major drawback of these solutions is the presence of propagation effects which produce the loss of the information associated to the discontinuities. On the other hand, the dicontinuities are very important for estimating precise optical flow fields, and detecting the shape of moving objects. In this paper, we propose a new solution based on variational techniques for optical flow estimation and regularization, which takes into account the discontinuities, and strongly reduces the related problems. The proposed method is called 'discontinuity-dependent variational solution'.

Keywords: computer vision, motion ananlysis, motion estimation, image flow, optical flow, regularization, discontinuities, smoothing

Motion analysis is based on the estimation of the velocity field which is the perspective projection of the real 3D velocity on the image plane. Basically, two approaches are discussed in the literature for the estimation of velocity on the image plane: the matching-based (correspondence) approach, and the gradient-based approach. In the first approach, local matching techniques are used to evaluate the displacements in sub-sequent frames for particular elements belonging to moving objects in the scene such as edges, corners, patterns, etc.[1–3]. The estimation of velocity vectors on the image plane by using the matching technique leads to obtain a sparse velocity field, since the estimation of displacement is only possible for some well-identifiable elements. On the other hand, where the matching problem is solved, the estimated velocity vectors are accurate.

The gradient-based approach begin with observations of brightness changes on the image plane, thus leading to the motion estimation of image brightness features[4–8]. This technique is based on the fact that the changes of image brightness $E(x(t), y(t), t)$ with respect to t can be denoted by:

$$\frac{dE}{dt} = \frac{\partial E}{\partial t} + \frac{\partial E}{\partial x}\frac{dx}{dt} + \frac{\partial E}{\partial y}\frac{dy}{dt} \tag{1}$$

If the image brightness of each point of the image is supposed to be stationary with respect to the time variable (i.e. $dE/dt = 0$), then the following expression holds:

$$E_t + E_x u + E_y v = 0 \tag{2}$$

where the abbreviation for partial derivatives of image brightness has been introduced, and u, v correspond to dx/dt, dy/dt, and represent the components of the local velocity vector $\mathbf{V}$ along the x and y directions, respectively. Equation (2) is usually called the Optical Flow Contraint (OFC).

The solutions of this equation are referred to as 'optical flow' or 'image flow'. In general, boundary and smoothness conditions are necessary for obtaining a computational solution for the OFC. However, these additional conditions can limit the correctness of the computed solutions.

In accordance with the previous discussion, the optical flow was defined by Horn and Schunck as the local velocity of the image grey value patterns, and

Department of Systems and Informatics, Faculty of Engineering, University of Florence, via di S. Marta 3, 50139 Florence, Italy

Paper received: 3 June 1992; revised paper received: 22 December 1992

0262–8856/93/070419–21

represents an approximation of the velocity field[5]. In general, the velocity field and the optical flow are not equal, and restrictive hypotheses are needed to make these two fields equal[9,10]. Nesi *et al.*[11] have pointed out that these two fields are the same if the objects in the scene have Lambertian surfaces, the motion is contained in a plane parallel to the image plane, the optical system is calibrated, and the scene is under isotropic illumination. These conditions are very restrictive with respect to conditions which are usually present in a real environment. On the other hand, the estimation of an approximated velocity field, such as an optical flow, can be very useful in many applications.

Nature of optical flow estimation problem

The problem of optical flow estimation from the OFC equation is not a well-posed problem in the sense of Hadanard[5,12,13], since the solution of the OFC equation is not unique, and for the presence of discontinuities. In addition, as can be seen by observing the OFC, the motion cannot be estimated if ∇E is close to zero, i.e. when the spatial changes in image brightness are small.

In the literature, another constraint has also been proposed for estimating optical flow, which is $d\nabla E/dt = 0$[8,14]. In the past, it has been pointed out that optical flow estimation by using the system of equations $d\nabla E/dt = 0$ is not generally an ill-posed problem[15] when $\det H \neq 0$ (where H is the Hessian of the image brightness). It should be noted that $\det H = E_{xx}E_{yy} - E_{xy}^2$, and hence it is therefore strongly related to the Gaussian curvature of image brightness. This means that optical flow estimation by using the $d\nabla E/dt = 0$ is either ill-conditioned when the curvature is low, or it is mainly present only along one direction. In such cases, the problem of optical flow etimation results to be mildly ill-posed (well behaved)[16]. This reasoning agrees with the fact that the matching-based algorithms only estimate reliable velocity vectors for well-identifiable elements such as corner points (where the Gaussian curvature is relevant), but they have problems when the element under matching is a linear edge with a strongly mono-dimensional curvature. It should be noted that by solving the system of equations $d\nabla E/dt = 0$ leads to obtain an optical flow which is theoretically different with respect to the one defined by the OFC. This is confirmed by the fact that the direct solution of the system of equations $d\nabla E/dt = 0$ does not usually verify the OFC equation.

In general, there are two main problems in estimating optical flow. The first consists in the presence of discontinuities in the local velocity, related to image brightness dscontinuities that are originated by the presence of noise, too crisp patterns, too large displacements, and occlusions beween moving objects. Discontinuities in optical flow fields are also present between the moving object and the stationary background along the so called 'object boundaries'. In the cases in which the optical flow is estimated by using $d\nabla E/dt = 0$, the presence of discontinuities in the optical flow fields makes the problem of optical flow estimation strongly ill-conditioned[15]. Generally speaking, this difficulty can be partially overcome by convolving the image with a 2D or 3D Gaussian smoothing operator transforming the problem into well-posed[14].

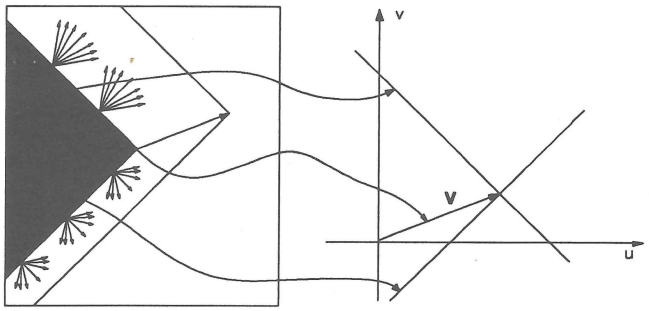

Figure 1. Instance of the problem of aperture and the associated constraint lines in the (u, v) space

The second problem is the so-called 'problem of aperture' which also exists in human vision. This is related to the impossibility of unequivocally recovering the motion direction if the object is observed through an aperture smaller than the object itself. In this context, the features on the object under observation (such as textures – patterns) are not enough to allow the perception of the transversal component of the object motion. This is coherent with human perception, which is not able to detect the true direction of the velocity of an object if it does not have enough references, such as a pattern or an edge curvature. In such cases, only the component of the velocity field which is parallel to the spatial gradient ∇E:

$$\mathbf{V}_{\perp} = -\frac{E_t}{\|\nabla E\|}\,\frac{\nabla E}{\|\nabla E\|} \tag{3}$$

can be estimated and perceived, where $dE/dt = 0$ and $\|\nabla E\| \neq 0$, are assumed.

As often pointed out by many researchers, the OFC can be seen as the equation of a line in the u, v plane. According to this, all the points of this line are possible solutions of the OFC[5]. A solution can be obtained as the intersection of the constraint lines in a neighbourhood where it is possible to define distinct constraints (such as at the edge boundary points in Figure 1). For this reason, the problem of aperture can be seen as an effect of the ill-conditioned nature of optical flow estimation.

In general, both the above-mentioned problems can be regarded as due to the ill-posed nature of the problem, since ill-posed problems have a condition number equal to ∞, and therefore the problems which are strongly ill-conditioned belong to the class of the ill-posed problems, and could be treated in the same manner[15].

In this paper, a new OFC-based solution for optical flow estimation is proposed. This solution is based on variational convergence to manage the ill-posed nature of the problem, and avoids the problems usually present when the classical regularization techniques are used. The mathematical bases of this approach were elaborated by Giorgi[17], and by Ambrosio and Tortorelli[18].

OPTICAL FLOW ESTIMATION TECHNIQUES

Two main gradient-based approaches for optical flow estimation can be found in the literature: *regularization* and *multiconstraint-based* approaches.

The *regularization-based* approaches consider optical flow estimation as an ill-posed problem in the sense of Hadamard[12,13], such as many other inverse problems in early-vision[15,19–23]. As in the classical regularization theory[15,24] these methods use a smoothness constraint to regularize the solution of OFC by minimizing a functional. In these functionals, the influence of the smoothness constraint is weighted with a positive constant. The functional can be minimized by using calculus of variations or stochastic relaxation (deterministic and stochastic regularization). Basically, these methods lead to iterative solutions, therefore the optical flow depends on the number of iterations involved.

The solutions based on regularization can be divided into two main classes: area- and countour-based solutions. The *regularization area-based* solutions lead to the evaluation of dense optical flow fields. The optical flow is called 'dense' when the estimation process yields the optical flow field also inside the objects under motion and not only on the contours. The results mainly depend on the number of iterations and on the weighting factor value.

Horn and Schunck[5] pointed out the ill-posed nature of the problem, and proposed a solution based on the minimization of the functional:

$$F = \int\int [(E_x u + E_y v + E_t)^2 + \alpha^2(u_x^2 + u_y^2 + v_x^2 + v_y^2)]\, dx\, dy \quad (14)$$

where the first term is the OFC (measure of the goodness of OFC approximation), the second is taken as a measure of departure from smoothness in optical flow, and α is a weighting factor that controls the degree of the smoothness constraint influence. The functional is minimized by using calculus of variations[25]. This approach leads to a system of two coupled differential equations obtained from the Euler equation, which can be decoupled and solved by using a discrete approximation. This method yields dense optical flow fields for the propagation of velocity values from the estimation points, and the depth of the propagation depends on both the number of iterations and the weight factor. The iterative process starts at the first iteration by estimating the optical flow vetors which are parallel to ∇E, and it continues by smoothing the field which is constrained by the OFC. Even though it converges to a minima, the iterative process does not converge to an optimal solution, since the lowest error in estimating the optical flow does not correspond to the iteration in which the process obtains the minimum of functional.

Terzopoulos[23] analysed the multigrid approach for solving Euler–Lagrange equations for some early-vision problems. Among these, a multigrid approach to the solution of Horn and Schunck[5] has been also presented. In general, the multigrid approach can be used for increasing the convergence velocity of low-frequency components (smooth modes) of the optical flow, while at the same time, high-frequency components (such as discontinuities) are strongly eliminated.

Schunck[26] presented the so-called 'line clustering' algorithm to estimate the optical flow in the presence of discontinuities. This technique works in the neighbourhood of the pixel under observation, and extracts a very probable velocity value by using a clustering technique. Moreover, an area-based algorithm is presented to regularize the optical flow estimated by means of the line clustering algorithm; this technique can be used only when the boundaries of the moving objects are known, and is based on the minimization of the functional:

$$F = \int\int [(u-\bar{u})^2 + (v-\bar{v})^2 + \alpha^2(\bar{u}_x^2 + \bar{u}_y^2 + \bar{v}_x^2 + \bar{v}_y^2)]\, dx\, dy$$

where $\bar{u}$ and $\bar{v}$ denote the estimated and smoothed optical flow fields. The first term can be seen as the deviation between the 'optical flow field estimated with line clustering' and the 'optical flow field estimated and smoothed'. The second term is the cost of the lack of smoothness in the solution. Minimizing this functional by using the calculus of variations yields two linear decoupled partial differential equations, and consequently an iterative solution can be easily obtained.

Yachida[27] used the same approach as Horn and Schunck to evaluate optical flow. In addition, a criterion for controlling the undesiderable propagation effects based on a measure of local brightness was reported.

Nagel[6] derived a different functional, and solutions were obtained in a closed form only at the corner points of an image. In the functional, a smoothing constraint which depends on the second-order partial derivatives of the image brightness has been used. Nagel and Enklemann[28] applied the solution proposed earlier[6] to every point of the image, and performed an accurate study of the properties of Nagel's orientation-dependent smoothness constraint. In the same paper, it was pointed out that the iterative solving process starts by estimating the velocity vectors in the corner points (where the velocity estimation can be made accurately), and continues with the propagation of estimates in the rest of the image.

Konrad and Dubois[29] presented two approaches for motion estimation that use the regularization based on Bayesian estimation. The first approach used a multi-grid algorithm to handle large displacements for a Maximum A Posteriori Probability (MAP) estimation of optical flow by simulated annealing. The second is an application of the Minimum Expected Cost (MEC) estimation.

Bertero *et al.*[15] and Poggio[19] analysed the ill-posed problems for early-vision. In this context, the bases of the regularization approach for optical flow estimation were also reported.

Schnörr[30] presented an approach to estimate optical flow and moving object shape at the same time. This method is based on the fact that *a priori* knowledge can be useful to improve the method proposed by Horn and Schunck[5]. In particular the ego-motion (3D motion of the observer) is given as known or estimated separately. The knowledge is used to decompose the optical flow in two domains, one for the ego-motion, the other for the moving object. The boundary between these two domains is defined as a closed curve. At this point an iterative process starts, to minimize the energy of domain separation, by modifying the closed curve, and estimating the optical flow fields in each domain. The optical flow in each domain is estimate by using the

algorithm of Horn and Schunck[5]. In Schnörr[30], only contexts having a single moving object with quite uniform motion have been fully investigated. Moreover, the process complexity depends on the number of the moving objects in the scene.

In the *regularization contour-based* solutions, the optical flow field is only evaluated on the edge of objects. This approach uses the OFC after the identification of the edges by means of an edge detection operator[2,31,32].

The *multiconstraint-based* approaches for optical flow estimation are based on the consideration that the condition $dF/dt = 0$ can be valid for any motion-invariant function F. This leads to the definition of a general constraint:

$$F_t + F_x u + F_y v = 0 \tag{5}$$

where many kinds of functions F can be used, such as contrast, entropy, average, variance, curvature, gradient magnitude, moments of local intensity, colour spectrum, images obtained with different light sources, etc. By using a set of these constraints, evaluated at the same point of the image, a solvable system of equations with u and v as unknowns can be obtained[33–35].

Some less general methods adopt other constraints having second-order partial derivatives of image brightness. These constaints can be seen as obtained by taking the derivative of OFC with respect to x, y or t[7,8,14].

To obtain smoother solutions, some researchers have considered that the constaints evaluated in the neighbourhood of the pixel under consideration represent the same velocity value, as a first approximation. In this way, a set of similar constraints in the neighbouring pixels can be used for building an over-determined system of equations. This assumption is valid only if the optical flow under observation is smooth[36,37].

Most of the previously mentioned techniques adopt an over-determined system of equations and obtain a solution by using the least-squares method. In such cases, the problem of optical flow estimation is not generally ill-posed, but can be strongly ill-conditioned depending on the presence of discontinuities and on the curvature of the image brightness. In general, this problem can be solved or simply attenuated by adopting (a) a pre-filtering, to regularize the data (sequence of images); (b) a large neighbourhood to collect a great number of constraints; and (c) a post-filtering of the estimated optical flow field, to smooth the solution. Such techniques can also be seen as a regularization method[15], but these lead to loss in resolution and make the estimated optical flow unsuitable for 3D object reconstruction.

VARIATIONAL CONVERGENCE FOR OPTICAL FLOW ESTIMATION

The main goal of the optical flow estimation is to obtain smooth optical flow fields on uniform regions, while maintaining the information on velocity vectors estimated on the boundaries profiles, and on the edges of the moving objects. Such optical flow can be profitably used for 3D motion estimation as well as for 3D object reconstruction, since the structural information related to discontinuities (i.e. the moving object boundaries and edges) is not destroyed. For this fact, the main problem in obtaining a precise optical flow field is to maintain the discontinuities.

As a general consideration, the multiconstraint-based approaches are much more sensitive to discontinuities than regularization-based techniques. This is mainly due to two facts: (i) the adoption of constraint equations with second-order partial derivatives of the image brightness (it is known that the derivation process exalts noise); (ii) the adoption of the least-squares technique to solve the over-determined system of constraint equations (the least-squares technique is not strongly robust with respect to the noise in data). A partial solution to these problems could be the adoption of a post-filtering action where the smoothness of the solution can be improved by increasing the area filter dimension, even though at the expense of a loss in resolution on object boundaries. In the regularization-based approaches, noise effects are reduced in the early iteration steps; however, during the iterative process, unacceptable optical flow estimates are obtained for the propagation of incorrect velocity vectors due to noise (estimated in the early iterations). Moreover, problems also occur in the presence of occlusions between moving objects, since the depth of propagation depends on both the number of iterations and the weighting factor.

In this paper, we proposed a solution for the estimation of smooth optical flow fields which maintains the information associated with discontinuities.

In the standard Tikhonov regulaization theory, the class of admissible solutions of an ill-posed problem is restricted to a Sobolev space of smooth functions[24]. Regularization with discontinuities needs a more general class of functions. Blake and Zisserman[38] proposed the weak membrane model to manage discontinuities. This method was generalized for other early-vision problems involving the regularization of ill-posed problem with discontinuities, such as visual reconstruction[39] and image segmentation[40]. In general, this variational method looks for a function $g(x, y)$ that minimizes the functional:

$$F(g) = \int\int (g(x, y) - d(x, y))^2 \, dx \, dy + \alpha^2 \int\int \| \nabla g(x, y) \|^2 \, dx \, dy + \beta^2 P$$

The first term is the measure of the error in the etimation, the second term is the smoothness constraint, and the last term is a measure of the discontinuities in $g(x, y)$. The penalty term ($\beta^2 P$) can be defined in many different ways[38]. In this case, the values of P are related to the presence of discontinuities. In this functional, α and β are the parameters of the problem. Blake and Zisserman discussed the meaning of these parameters in term of discontinuity detection, obtaining α as the scale factor and $T = \sqrt{2\beta^2/\alpha}$ as the threshold, for detecting the discontinuities. As the value of α increases, the effect of the smoothing factor (i.e. the second term) also increases, and so this value should be related to the signal-to-noise ratio. The velocity values which are higher than the threshold T are maintained, while the others are smoothed[38].

In general, this problem can be regarded as an

extension of the classical regularization method used for managing the presence of discontinuities. Even though it has not yet been proved that this problem is well-posed, however, the results obtained lead to the supposition that this is true[39]. In addition, Blake and Zisserman demonstrated that in two important cases (i.e. for isolated discontinuities and for a pair of interacting discontinuities which are closer than a certain factor), their graduated non-convexity method finds the global minima, and is therefore correct[38].

Recently, a new concept of convergence for sequence of functionals has appeared in mathematical analysis[17,18,40,41]. This particular therory of variational convergence, called Γ-convergence[17], leads to determining, from a functional $F(g)$, a sequence of k-dependent functionals $F_k(g)$, which minimized lead to a solution for the minimization problem that is also valued for the functional $F(g)$ for k that tends to infinity.

A sequence of functionals that approximates the functional $F(g)$ in the sense of the Γ-convergence is:

$$F_k(g, z) = \iint \Big[(g(x, y) - d(x, y))^2 + \alpha^2 z^2 \| \nabla g(x, y) \|^2 + \beta^2 \Big(\frac{\| \nabla z \|^2}{k} + \frac{k(1-z)^2}{4} \Big) \Big] dx\, dy$$

In this way, the problem is more tractable, but the additional variable z has been inserted. This variable is

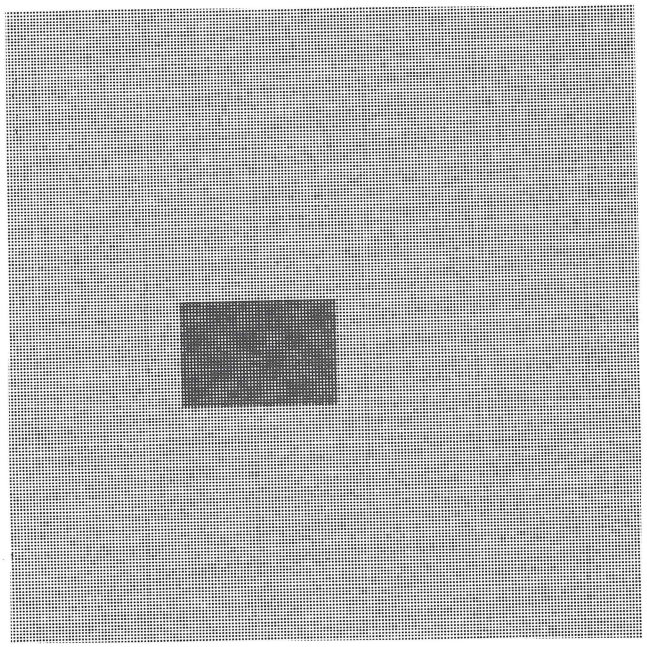

2

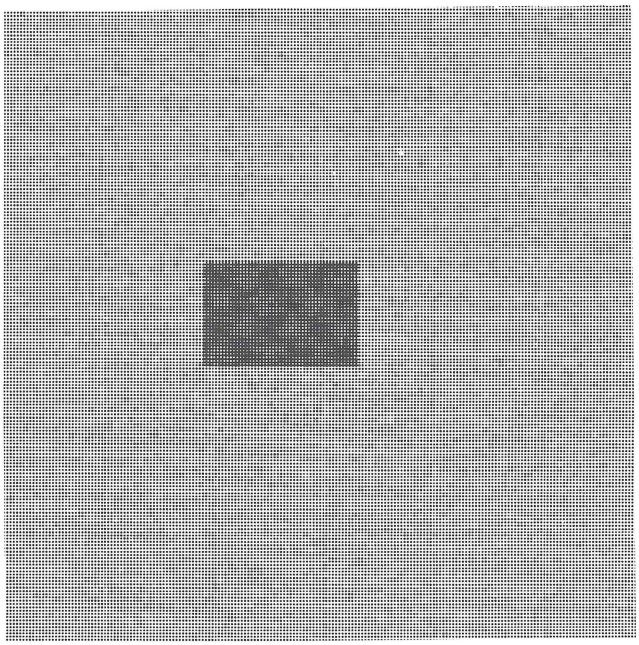

6

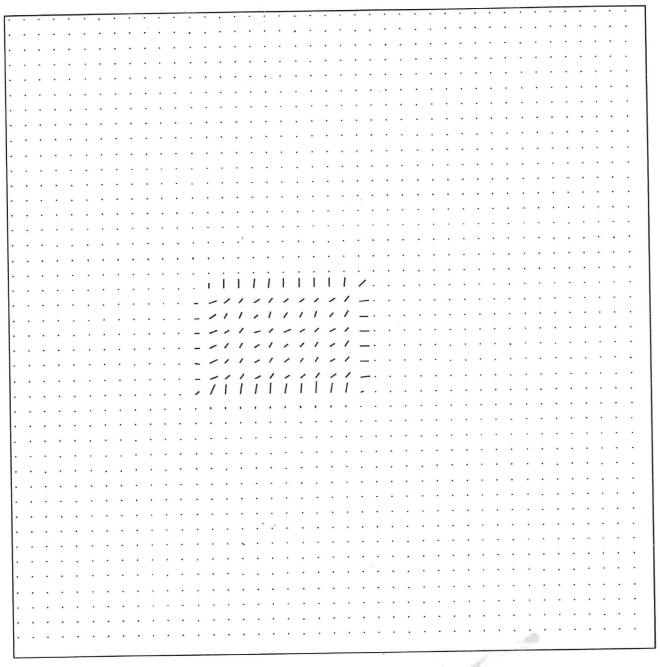

1

Figure 2. Sequence of images where an object with a superimposed plaid pattern is moving at 45° with respect to the x-*axis. Moreover, 20% Gaussian noise was added to whole image (2nd and 6th frame 128 × 128 image resolution). Optical flow estimated at the first iteration*

related to the presence of discontinuities, and has a variation range between 0 and 1. This function can be considered a control variable which assumes the value 0 in presence of discontinuities, and it is close to 1 in smooth regions, when k is large. At this regard, Ambrosio and Tortorelli[18] proved that the sequence of these functional $F_k(g, z)$ converges to the sum of the last two terms of the functional $F(g)$ with k tending towards infinity. In addition, the functional is continuous if the function that implements the estimation error is continuous. Moreover, the Γ-limit of the sequence $F_k(g, z)$ does not depend on the variable z, as shown elsewhere[39].

In this paper, it is shown that this technique can also be profitably used for motion estimation, where in this case the functional F_k takes the form:

$$F_k(u, v, z) = \iint \left[(E_x u + E_y v + E_t)^2 + \alpha^2 z^2 (u_x^2 + u_y^2 + v_x^2 + v_y^2) + \beta^2 \left(\frac{\|\nabla z\|^2}{k} + \frac{k(1-z)^2}{4} \right) \right] dx\, dy$$

where the first term is the optical flow constraint; the second is the smoothness constraint adopted by Horn and Schunck[5] multiplied by the control function z^2, and the last term is the penalty function that takes the discontinuities into account, and is called the 'discontinuity-dependent penalty constraint'.

The solution of the defined functional by the calculus of variations leads to three coupled non-linear partial differential equations:

$$\alpha^2 z^2 (u_{xx} + u_{yy}) + 2\alpha^2 z (u_x z_x + u_y z_y) - E_x^2 u - E_x E_y v - E_x E_t = 0$$

$$\alpha^2 z^2 (v_{xx} + v_{yy}) + 2\alpha^2 z (v_x z_x + v_y z_y) - E_x E_y u - E_y^2 v - E_y E_t = 0$$

$$\frac{\beta^2}{k} (z_{xx} + z_{yy}) + \frac{\beta^2 k}{4} (1 - z) - \alpha^2 z (u_x^2 + u_y^2 + v_x^2 + v_y^2) = 0$$

These Euler equations can be solved by using natural boundary conditions. By discretizing the above equations, with the finite difference method, the following coupled equations are obtained:

$$4\alpha^2 z_{i,j,t}^2 (\bar{u}_{i,j,t} - u_{i,j,t}) + 2\alpha^2 z_{i,j,t} (u_{xi,j,t} z_{xi,j,t} + u_{yi,j,t} z_{yi,j,t}) - E_{xi,j,t}^2 u_{i,j,t} - E_{xi,j,t} E_{yi,j,t} v_{i,j,t} - \mathrm{E}_{\mathrm{xi},j,t} E_{ti,j,t} = 0 \quad (6)$$

$$4\alpha^2 z_{i,j,t}^2 (\bar{v}_{i,j,t} - v_{i,j,t}) + 2\alpha^2 z_{i,j,t} (v_{xi,j,t} z_{xi,j,t} + v_{yi,j,t} z_{yi,j,t}) - E_{xi,j,t} E_{yi,j,t} u_{i,j,t} - \mathrm{E}_{yi,j,t}^2 v_{i,j,t} - \mathrm{E}_{\mathrm{yi},j,t} E_{ti,j,t} = 0 \quad (7)$$

$$4 \frac{\beta^2}{k} (\bar{z}_{i,j,t} - z_{i,j,t}) + \frac{\beta^2 k}{4} (1 - z_{i,j,t}) - \alpha^2 z_{i,j,t} (u_{xi,j,t}^2 + u_{yi,j,t}^2 + v_{xi,j,t}^2 + v_{yi,j,t}^2) = 0$$

where the follow approximations are used:

$$E_{xi,j,t} = (E_{i+1,j,t} - E_{i-1,j,t})/2$$

$$E_{yi,j,t} = (E_{i,j+1,t} - E_{i,j-1,t})/2$$

$$E_{ti,j,t} = (E_{i,j,t+1} - E_{i,j,t-1})/2$$

and:

$$u_{xxi,j,t} + u_{yyi,j,t} = 4(\bar{u}_{i,j,t} - u_{i,j,t})$$

with:

$$\bar{u}_{i,j,t} = (u_{i+1,j,t} + u_{i-1,j,t} + u_{i,j+1,t} + u_{i,j-1,t})/4$$

that can be regarded as the average in the neighbours of the point located by (i, j) at time t, and:

$$u_{xi,j,t} = (u_{i+1,j,t} - u_{i-1,j,t})/2$$

$$u_{yi,j,t} = (u_{i,j+1,t} - u_{i,j-1,t})/2$$

Analogously for the variables v and z. An explicit iterative solution can be obtained from the discrete version of these equations by using the method of Jacobi[42]:

$$u_{i,j,t}^{n+1} = \frac{4\alpha^2 (z_{i,j,t}^n)^2 \bar{u}_{i,j,t}^n - E_{xi,j,t} E_{yi,j,t} v_{i,j,t}^n - E_{xi,j,t} E_{ti,j,t} + 2\alpha^2 z_{i,j,t}^n (u_{xi,j,t}^n z_{xi,j,t}^n + u_{yi,j,t}^n z_{yi,j,t}^n)}{4\alpha^2 (z_{i,j,t}^n)^2 + E_{xi,j,t}^2}$$

$$v_{i,j,t}^{n+1} = \frac{4\alpha^2 (z_{i,j,t}^n)^2 \bar{v}_{i,j,t}^n - E_{xi,j,t} E_{yi,j,t} u_{i,j,t}^n - E_{yi,j,t} E_{ti,j,t} + 2\alpha^2 z_{i,j,t}^n (v_{xi,j,t}^n z_{xi,j,t}^n + v_{yi,j,t}^n z_{yi,j,t}^n)}{4\alpha^2 (z_{i,j,t}^n)^2 + E_{yi,j,t}^2}$$

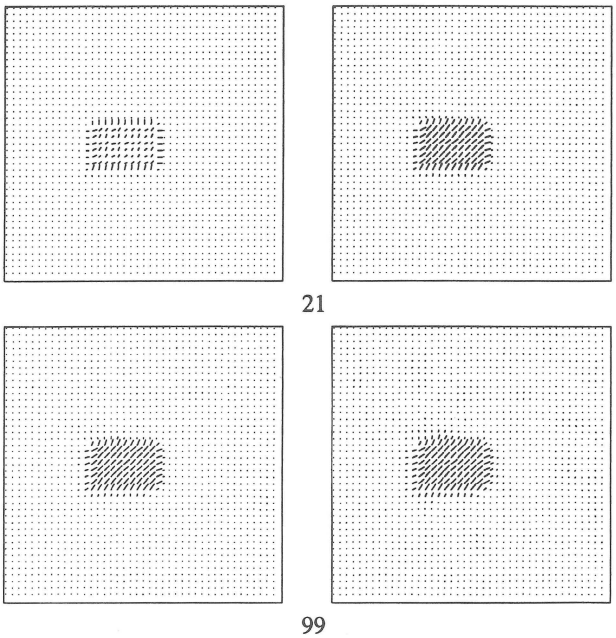

Figure 3. Optical flow estimation referred to the 5th frame of the sequence in Figure 2 ($\alpha = 3$, $\beta = 1.3$, k = 3) (iterations: 3, 21, 33, 99)

$$z^{n+1}_{i,j,t} = \frac{\bar{z}^{n}_{i,j,t}16 + k^2}{k^2 + 4k(\alpha^2/\beta^2)((u^{n}_{xi,j,t})^2 + (u^{n}_{yi,j,t}{}^2 + (v^{n}_{xi,j,t})^2 + (v^{n}_{yi,j,t})^2) + 16}$$

where n is the iteration number.

The convergence velocity of the iterative solution defined by these coupled equations is not very fast. Faster and smoother estimates are obtained by using the averaged values $\bar{u}^{n}_{i,j,t}$, $\bar{v}^{n}_{i,j,t}$, and $\bar{z}^{n}_{i,j,t}$ instead of the local values $u^{n}_{i,j,t}$, $v^{n}_{i,j,t}$, $z^{n}_{i,j,t}$ in some points of the expressions for $u^{n+1}_{i,j,t}$, and $v^{n+1}_{i,j,t}$, obtaining:

$$u^{n+1}_{i,j,t} = \frac{4\alpha^2(\bar{z}^{n}_{i,j,t})^2\bar{u}^{n}_{i,j,t} - E_{xi,j,t}E_{yi,j,t}\bar{v}^{n}_{i,j,t} - E_{xi,j,t}E_{ti,j,t} + 2\alpha^2\bar{z}^{n}_{i,j,t}(u^{n}_{xi,j,t}z^{n}_{xi,j,t} + u^{n}_{yi,j,t}z^{n}_{yi,j,t})}{4\alpha^2(\bar{z}^{n}_{i,j,t})^2 + E^2_{xi,j,t}}$$

$$v^{n+1}_{i,j,t} = \frac{4\alpha^2(\bar{z}^{n}_{i,j,t})^2\bar{v}^{n}_{i,j,t} - E_{xi,j,t}E_{yi,j,t}\bar{u}^{n}_{i,j,t} - E_{yi,j,t}E_{ti,j,t} + 2\alpha^2\bar{z}^{n}_{i,j,t}(v^{n}_{xi,j,t}z^{n}_{xi,j,t} + v^{n}_{yi,j,t}z^{n}_{yi,j,t})}{4\alpha^2(\bar{z}^{n}_{i,j,t})^2 + E^2_{yi,j,t}}$$

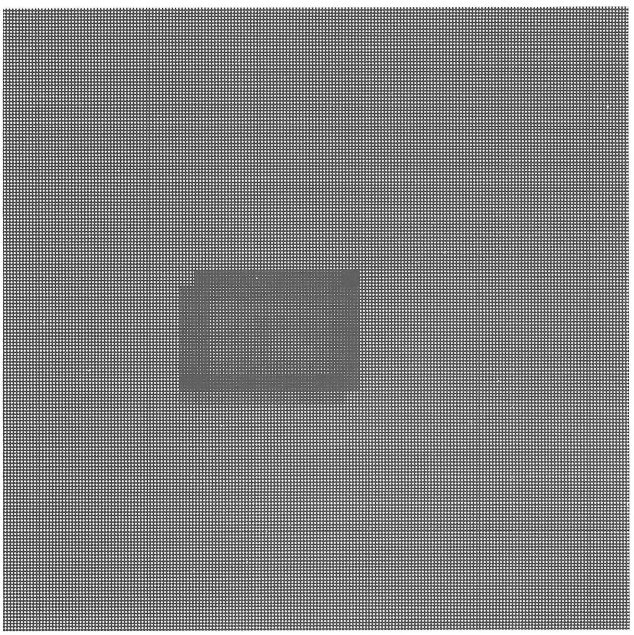

3

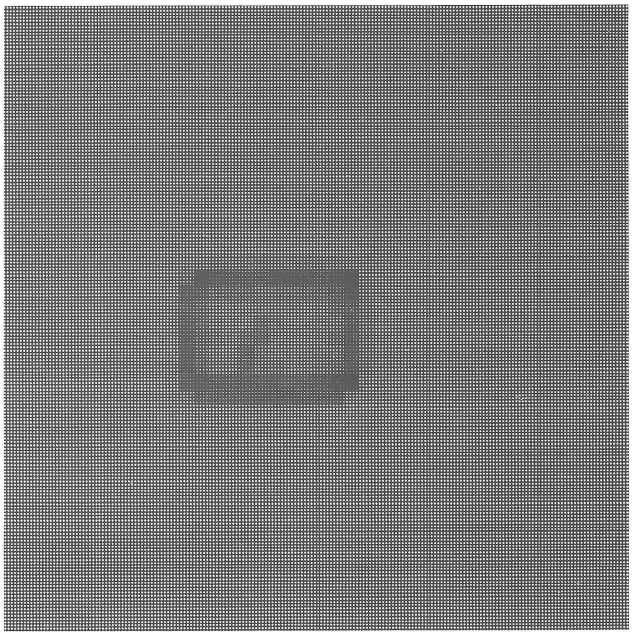

21

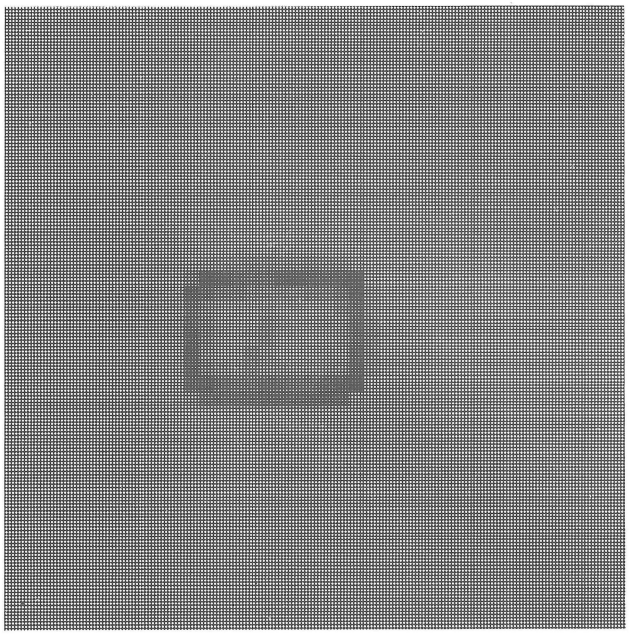

33

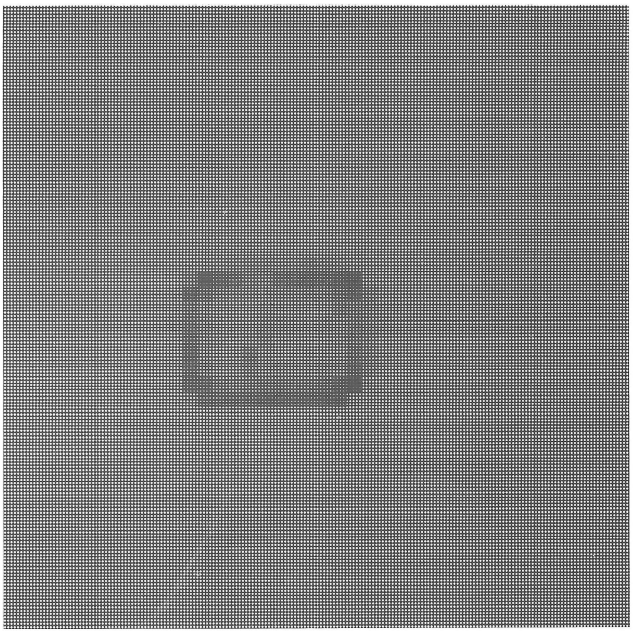

99

Figure 4. Maps of the control function z corresponding to the optical flow fields shown in Figure 3 (iterations: 3, 21, 33, 99)

This method yields a dense optical flow for the propagation of velocity values in the regions where the discontinuities are lower than the threshold $\sqrt{2\beta^2/\alpha}$. The value of α has only effect in those regions, since the control function inhibits the smoothing action where there are discontinuities. This mechanism maintains the profiles of the moving objects and improves the signal-to-noise ratio with respect to the solutions not using the discontinuity-dependent penalty constraint. By using the solution presented, the propagation depth depends on the number of iterations, on the weight factor, and on the presence of discontinuities (being controlled by z). This avoids problems of the loss of moving object boundaries where one moving object occludes another. In addition, the iterative process can be ueful for shortening a temporal sequence of estimation processes, since a guess for the optical flow values (estimated at time t) is available from the previous time-step (at $t-1$).

EXPERIMENTAL RESULTS

The analysis is carried out by comparing the estimates obtained through regularization-based solutions with the discontinuity-dependent penalty constraint (described in the previous section) with respect to the solutions obtained without this constraint. The latter solution is taken as a representative of the classical regularization approaches[5,28,43], and corresponds, at least in prinicple, to the solution proposed by Horn and Schunck[5]. The multiconstraint-based solutions are not taken into consideration, since they present too different a behaviour with respect to the regularization-based solutions, and their results are usually very sensitive to discontinuities. The behaviour of the algorithms is analysed with reference to sequences of both synthetic and real senes. The choice of α, β, k parameters is made on the basis of suggestions proposed by Blake and Zisserman[38].

In the tests presented, the estimates of the optical flow fields were obtained by using a grid equal to one image pixel (1×1). To make the optical flow fields more readable, these are shown with a grid of 3×3 obtained from the 1×1 grid by averaging the estimated optical flow values in a 3×3 neighbourhood around the point of the dense grid. In addition, for the iterative solutions obtained using the discontinuity-dependent penalty constraint, the starting value for the control variable z is equal to 1 everywhere. This means that the absence of discontinuity detection is assumed at the first iteration.

Discontinuities

Figure 2 shows a test sequence where a quadrilateral with a superimposed plaid pattern is moving with translational motion at 45° with respect to the x-axis, and is used to test the algorithm with respect to translational motion. The object with a plaid pattern

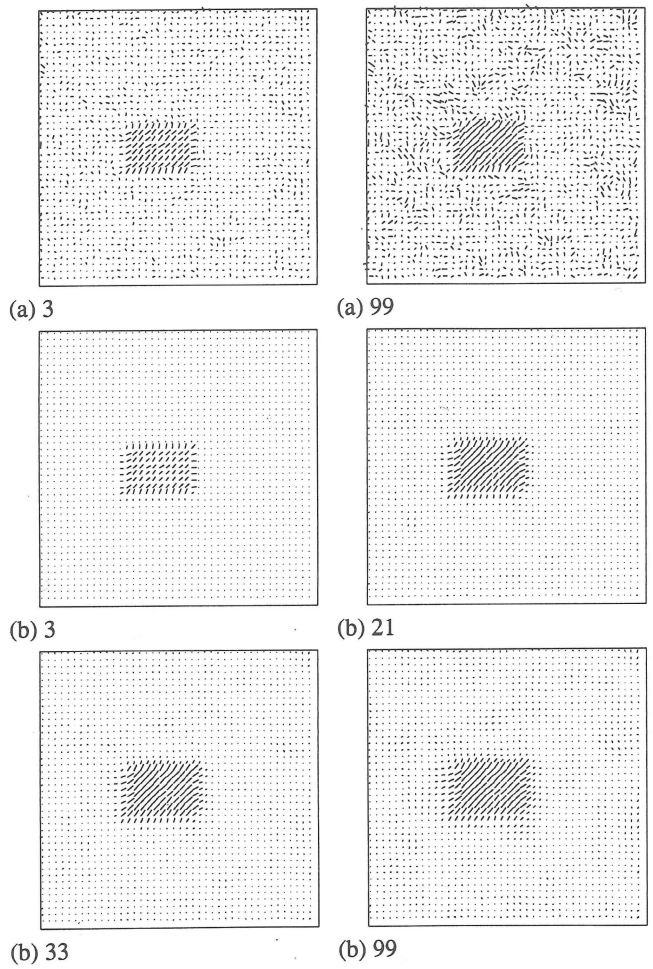

Figure 5. Optical flow estimation referred to the 5th frame of the sequence in Figure 2 obtained without penalty constraint. (a) $\alpha = 0.6$, iterations: 3 and 9; (b) $\alpha = 3$, iterations: 3, 21, 33, 99

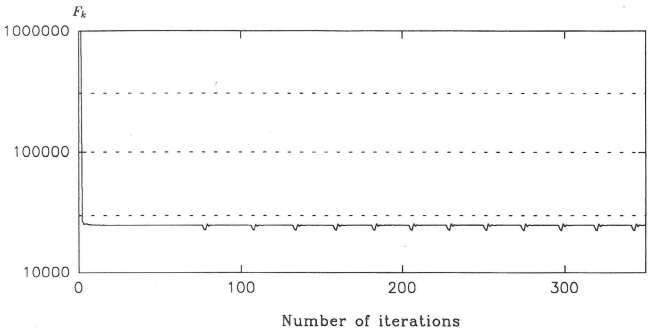

Figure 6. Values of the functional F_k with the discontinuity-dependent penalty constraint as a function of the iteration number n

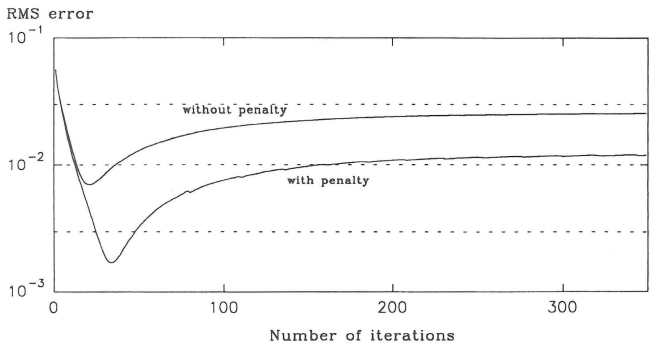

Figure 7. Values of the RMS errors in estimating optical flow as functions of the iteration number n (for the image sequence presented in Figure 2) for the cases with and without discontinuity-dependent penalty constraint

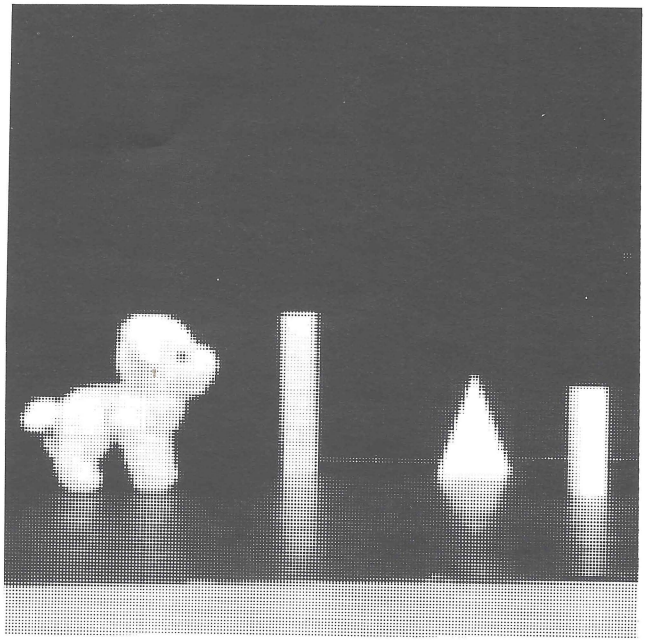

3

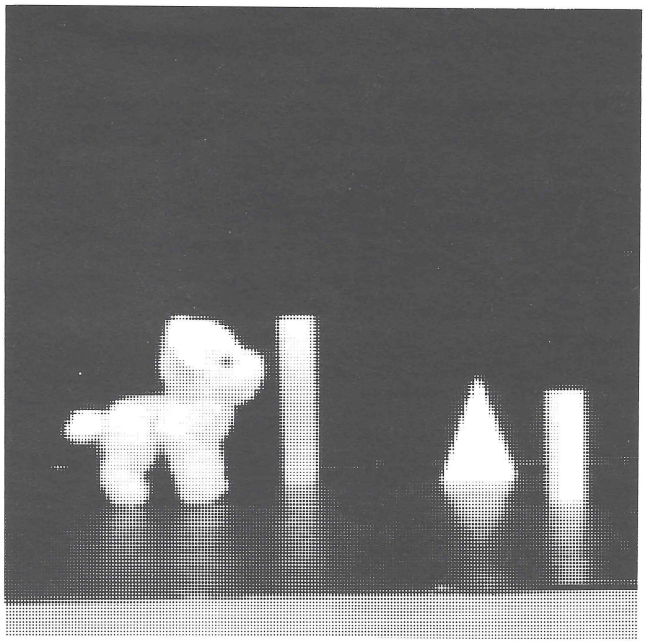

10

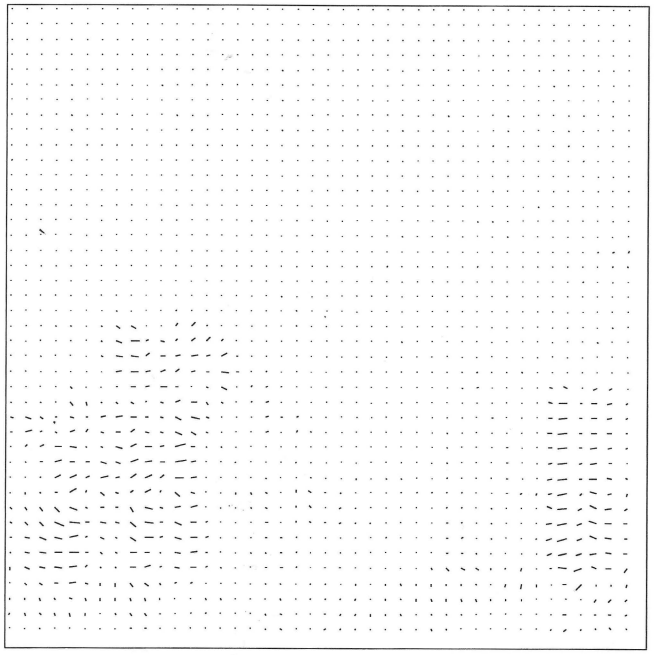

1

Figure 8. Scene where two real objects are moving in translational motion along the x*-axis (3rd and 10th frame, 128 × 128 image resolution). Optical flow estimated at the first iteration*

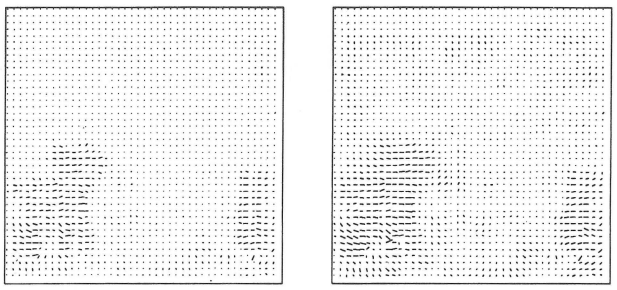

6 42

Figure 9. Optical flow estimation using the discontinuity-dependent penalty constraint on the 5th frame of the sequence in Figure 8 (iterations: 6, 42) ($\alpha =$, $\beta = 1.3$, k = 3)

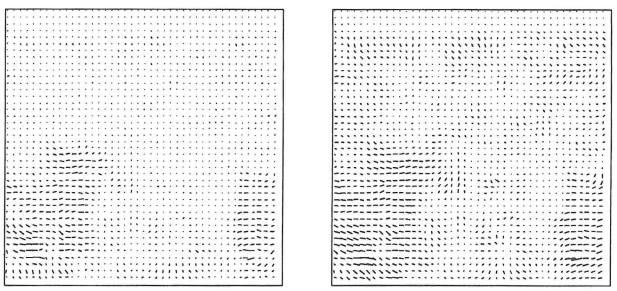

6 42

Figure 10. Optical flow estimation on the 5th frame of the sequence in Figure 8 obtained without penalty constraint ($\alpha = 3$, iterations: 6, 42)

was obtained by superimposing two sinusoidal patterns with orthogonal directions on the object grey level. Moreoever, 20% of Gaussian noise was added to the images to test the algorithm's response in the presence of discontinuities due to noise. Due to the presence of the plaid pattern on the moving object, the optical flow is also estimated inside the object's boundaries for the solutions presented (see Figures 3 and 5). In Figure 2 the optical flow obtained after the first iteration is also presented; this has been reported since it represents the initial field for solutions both with and without penalty constraint.

In Figure 3 some optical flow estimates at different iteration numbers obtained using the discontinuity-depedendent penalty constraint on the image sequence presented in Figure 2 are reported. This solution was obtained with $\alpha = 3$, $\beta = 1.3$ and $k = 3$ (i.e. $T = 1.06$). In Figure 4, the respective maps of the control function z for the same iterations proposed in Figure 3 are shown. In the maps of the control function z, the values which are close to zero have a darker grey level, while a medium grey level represents the 1 value. From these figures it can be seen that the control function tends to select the boundaries of the moving object by controlling the regularization of discontinuities. The adoption of the discontinuity-dependent penalty constaint is very useful to avoid the propagation effect (see Figure 3) that occurs in the solution without penalty constraint (see Figure 5). This very appreciable effect does not disturb regularization inside the boundaries of the moving object very much, as can be seen by comparing Figure 3 with Figure 5 for the same iteration number.

In Figure 5, optical flow fields estimated without the discontinuity-dependent penalty constraint for two different values of α are reported. In the solution without the penalty constraint, low values of α may not be sufficient to reject noise. However, when high values of α are used, incorrect velocity vectors appear as the iteration number increases. These incorrect vectors grow (during the iterative process) around small velocity vectors which are due to noise in the early iterations (see Figure 5). This effect is greatly reduced by the discontinuity-dependent penalty constraint, as shown in Figure 3, even if the α value is the same. With the classical regularization technique, smoother solutions can be obtained by increasing the value of α, but as a consequence the undesirable propagation effect smoothing the boundries of the moving objects also increases (see Figure 5). These two contradictory factors can be controlled by using the discontinuity-depended constraint, where the iterative process produces good solutions, since it does not destroy the correct results obtained in the early iterations (see Figure 3).

In Figure 6, the values of the functional F_k with the penalty constraint as a function of the iteration number n are reported. In Figure 7, RMS error values for the optical flow fields estimated by minimizing the functional F_k with and without penalty constraints are presented, referring to the optical flow estimates for the sequence in Figure 2. It can be seen that the lowest error is obtained in a few iterations (21st iteration), but for the same number of iterations, the solution with the penalty constraint produces an optical flow with a lower error. In addition, the solution with the penalty constraint obtains the lowest error at the 33rd iteration, which is about 10 times lower than the error obtainable by the solution without the penalty constraint. It should be noted that the plots were evaluated using the same α value for both solutions. Moreover, by using the solution with the penalty constraint, it is possible to increase the α value without increasing the propagation effect if the value of threshold T is maintained as a constant.

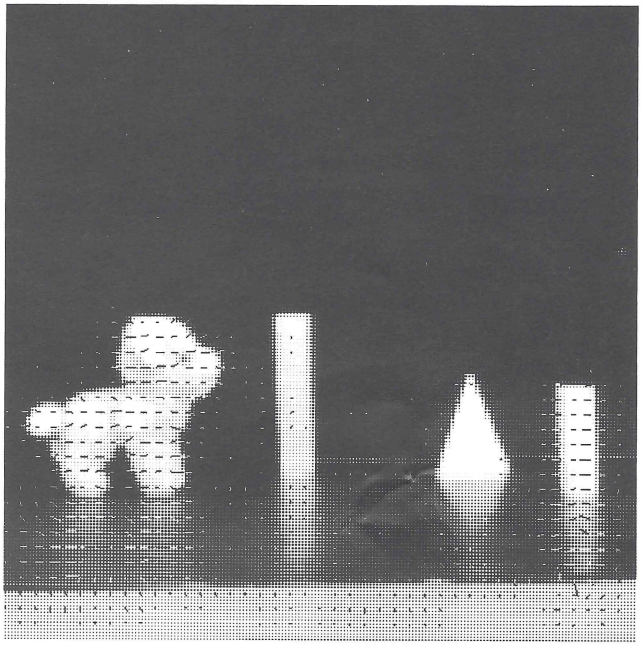

(a) 6

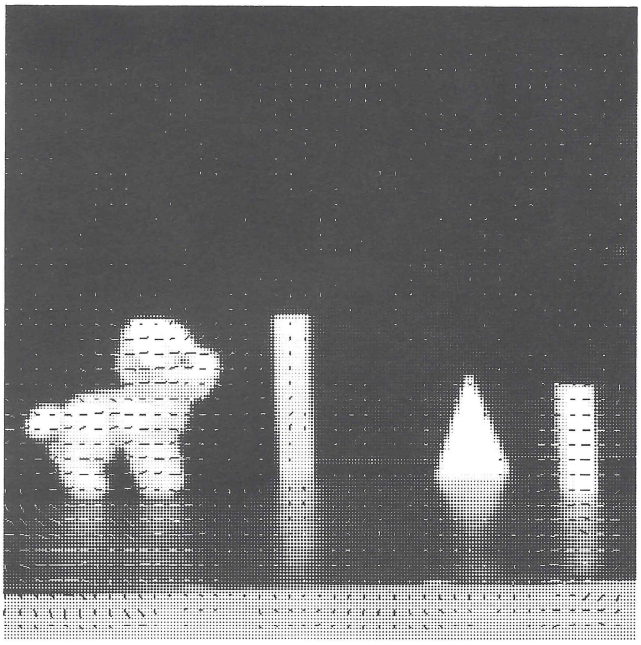

(b) 6

Figure 11. Optical flow fields (6th iteration) superimposed on the 5th frame of the sequence in Figure 8, obtained using the solutions (a) with the discontinuity-dependent penalty constraint ($\alpha = 3$, $\beta = 1.3$, $k = 3$), and (b) without the penalty constraint ($\alpha = 3$)

In Figure 8 a sequence were two toys moving (on a partially reflective plane) in opposite directions is reported. The optical flow fields estimated at different iteration numbers using the presented algorithm on this test sequence are reported in Figure 9. Figure 10 illustrates corresponding results (for the same α value) obtained without the penalty constraint. It can also be noted that in this case, the discontinuity-dependent solution avoids the propagation effect and increases the signal-to-noise ratio. In particular, the solution without the penalty constraint tends to propagate estimates starting also from incorrect velocity vectors caused by noise. The differences between the two types of solution are particularly evident in Figure 11, where the optical flow fields are superimposed on the reference image. In this figure, velocity vectors lower than 0.001 are not drawn, while the largest velocity vector is close to 1.

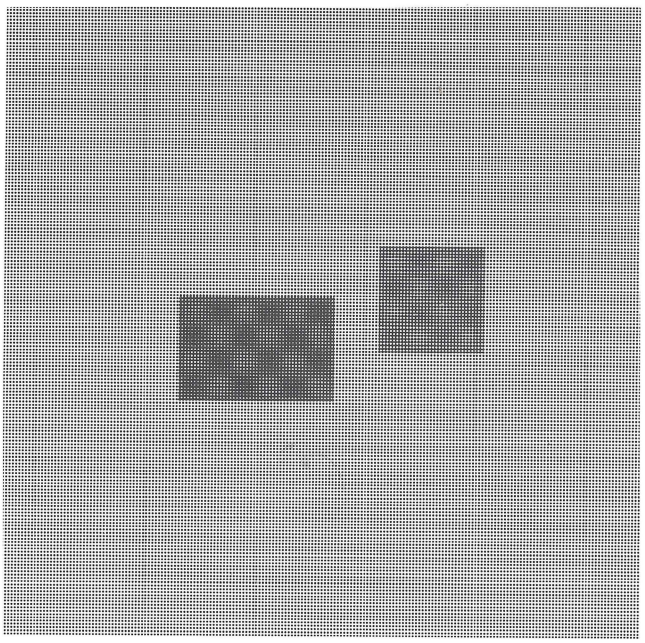

1

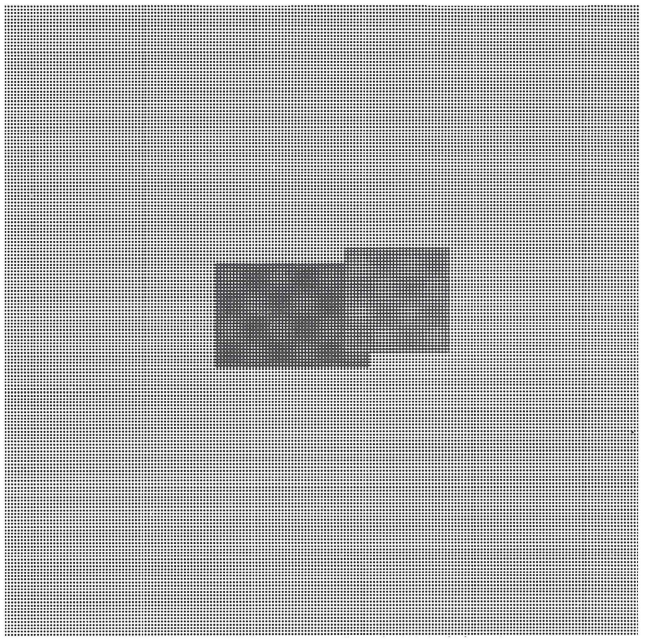

8

Figure 12. Sequence of images where two objects with a superimposed plaid pattern are moving in opposite directions (at 180° and 45; with respect to the x-axis, respectively). (1st and 8th frame, 128 × 128 image resolution)

The synthetic sequence in Figure 12 shows two objects with a superimposed plaid pattern moving in different directions. This sequence was used to test the behaviour of the proposed solution in the presence of discontinuities due to occlusions among moving objects. Usually, solutions obtained by multiconstraint-based approaches produce less satisfactory velocity estimates at points which are close to the occlusion profile between the moving objects. In solutions obtained by the traditional regularization-based approach, the dicontinuities are strongly reduced. Unfortunately, these methods are affected by the undesiderable effect of propagation, which consists in the loss of object boundaries on the occluding profiles (see Figure 15). Also in these cases, the presented solution, which adopts the discontinuity-dependent penalty constraint, produces good results, maintaining the profiles of the moving objects even in the presence of object occlusion (see Figure 13 and the respective z maps in Figure 14).

The sequence in Figure 16 shows a very noisy real outdoor environment where two vehicles are moving with different 3D motions. This sequence was used to test the algorithm's behaviour with respect to real imagery. The responses of the algorithm are reported in Figure 17. In this case, a high value for the β parameters ($\alpha = 3$, $\beta = 4$, $k = 4$) was used for estimating the optical flow by using the solution with the penalty constraint, because the test image is very noisy. Since the moving objects in this test case present a real 3D motion, the control function also selects the discontinuities along the moving edges. As can be seen

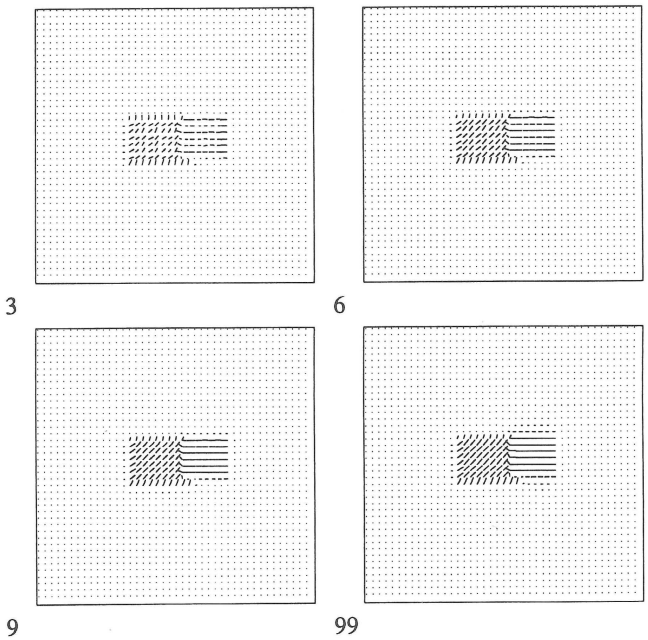

3 6

9 99

Figure 13. Optical flow estimation on the 8th frame of the sequence in Figure 12 (iterations: 3, 6, 9, 99) ($\alpha = 3$, $\beta = 1.3$, $k = 5$)

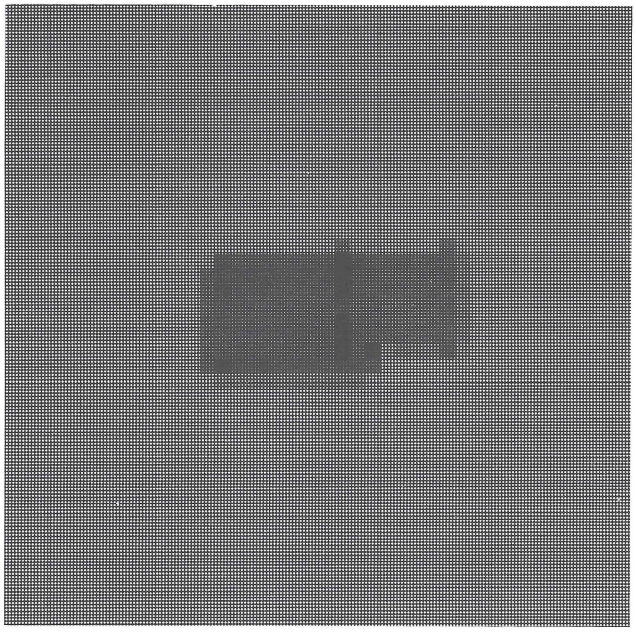

3

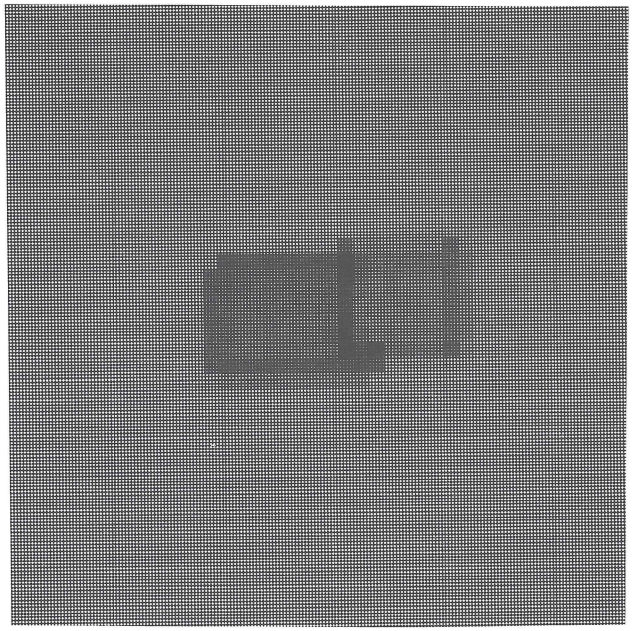

6

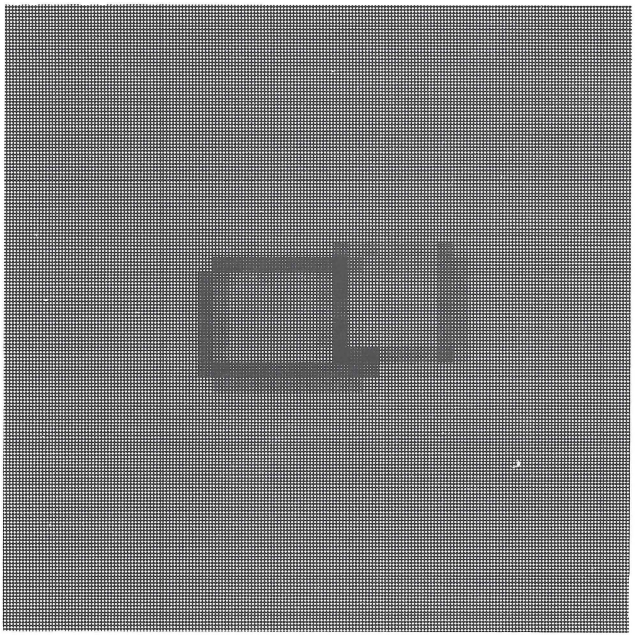

9

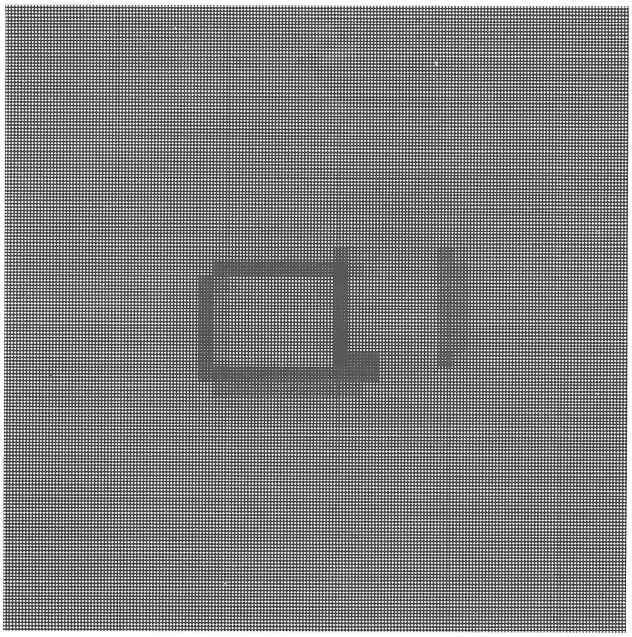

99

Figure 14. Maps of the control function z corresponding to the optical flow fields shown in Figure 13 (iterations: 3, 6, 9, 99)

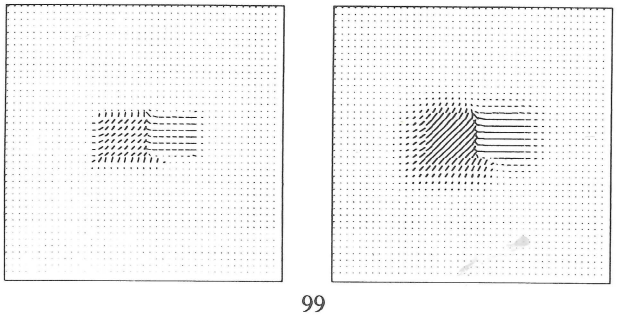

3 99

Figure 15. Optical flow estimation on the 8th frame of the sequence in Figure 12 obtained using the solution without the penalty constraint ($\alpha = 3$, iterations: 3, 99)

1

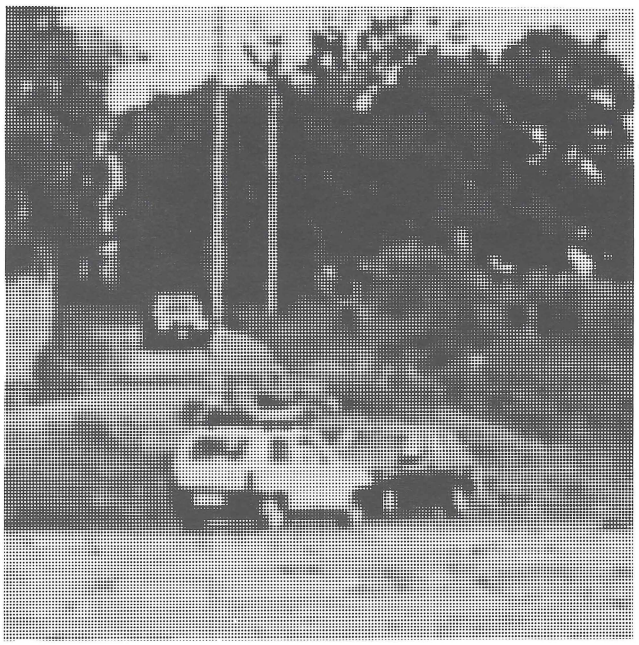

10

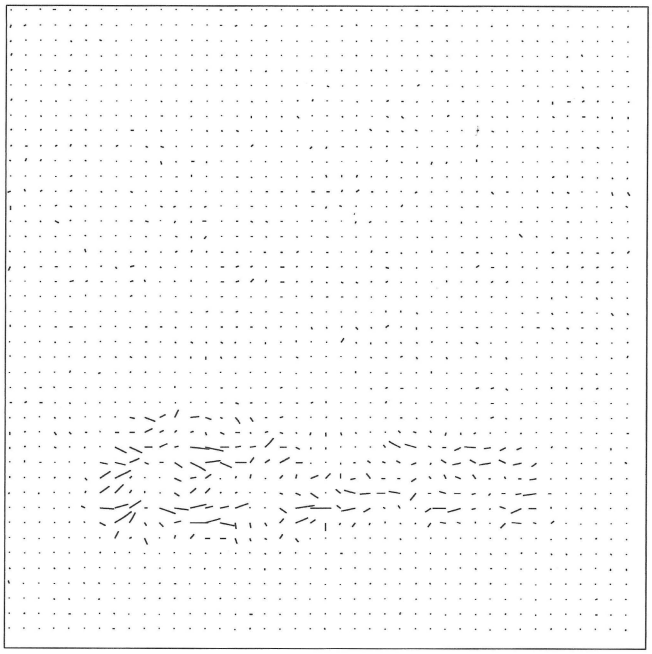

1

Figure 16. Sequence of a real environment where two vehicles are moving with different 3D motions (1st and 10th frame, 128 × 128 image resolution). Optical flow estimated at the first iteration

in Figure 17, the discontinuity-dependent solution, also in this case, avoids the propagation effect and increases the signal-to-noise ratio. In Figure 18 the optical flow fields for both solutions are superimposed to the reference image.

In Figure 19 the optical flow field estimated using the discontinuity-dependent penalty constraint superimposed on the reference image is shown. In this case, the image sequence is taken by using a TV-camera mounted on a vehicle which is moving on the road. For this reason, each object in the background is moving with respect to the camera. In addition, there is another veicle (i.e. a car) which is moving along the road in the opposite direction. The estimated optical flow presents velocity vectors with different directions for different moving objects. The corresponding z map shows the detected discontinuities; these have been used in the optical flow estimation process to avoid the propagation effect, preserving the object shapes.

Problem of aperture

As pointed out in the introduction, the problem of aperture is related to the ill-posed nature of the optical flow estimation problem. In particular, the obtainable results depend on the kind of constraint used, and on the image brightness curvature. The multiconstraint-based approaches which define an over-determined system of equations can have several intersections among the adopted constraint lines in a neighbourhood. In such cases, the robustness of the system of equations with respect to the ill-conditioning depends on the kind of constraints used to define the system.

A test sequence in which a sinusoidal transversal pattern moves in a translational motion has been used to study the aperture problem (i.e. very similar to the famous 'barber pole' sequence) (see Figure 20). In every point inside the aperture the Gaussian curvature of the image brightness pattern is equal to zero, even if the second-order partial derivatives of the image brightness are different from zero. This means that the Gaussian curvature is equal to zero in every point of the image except for the points on the aperture boundary.

Like many other regularization-based solutions[5,44]

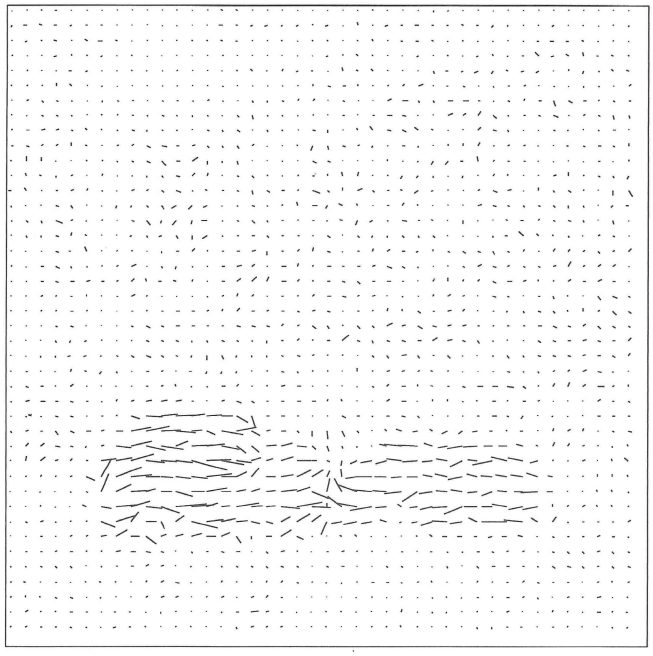

(a) 40

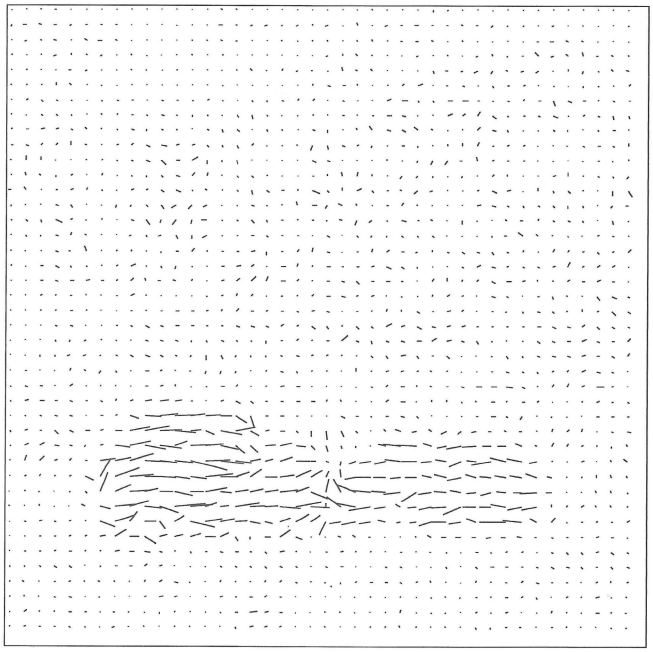

(a) 100

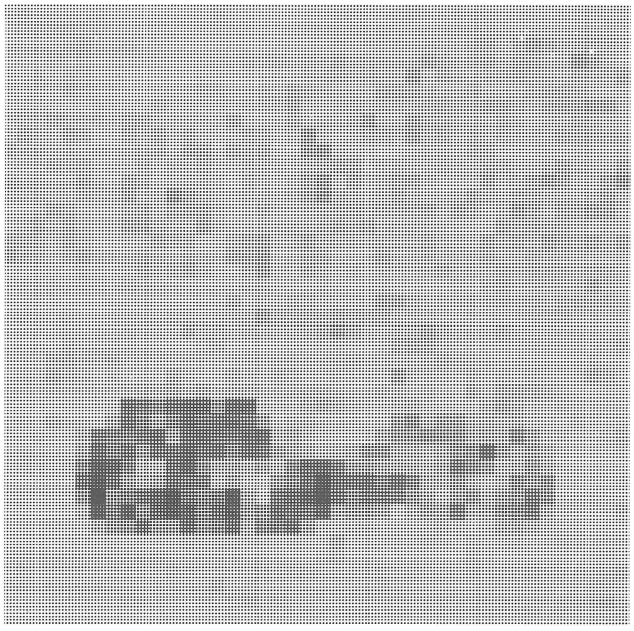

(a) z at the 20th iteration

Figure 17. Optical flow fields (iterations: 40, 100) on the 2nd frame of the sequence in Figure 16 obtained using the solutions: (a) with the discontinuity-dependent penalty constraint ($\alpha = 3$, $\beta = 4$, $k = 4$);

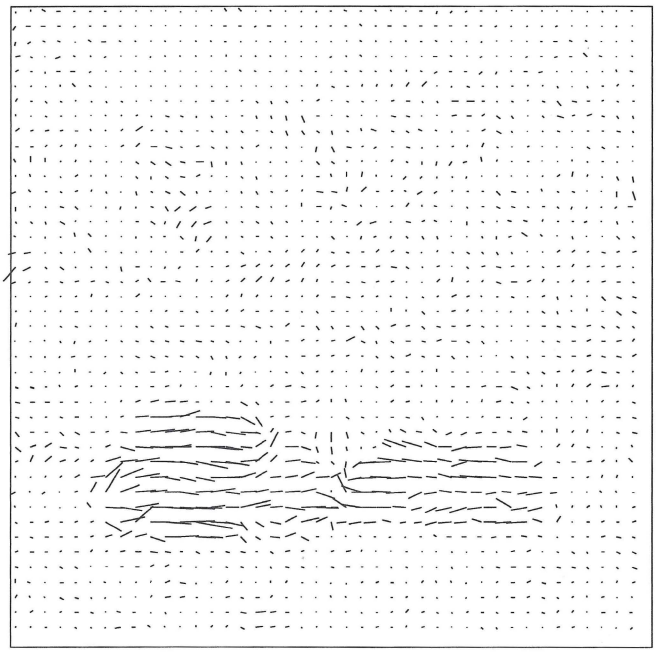

(b) 40

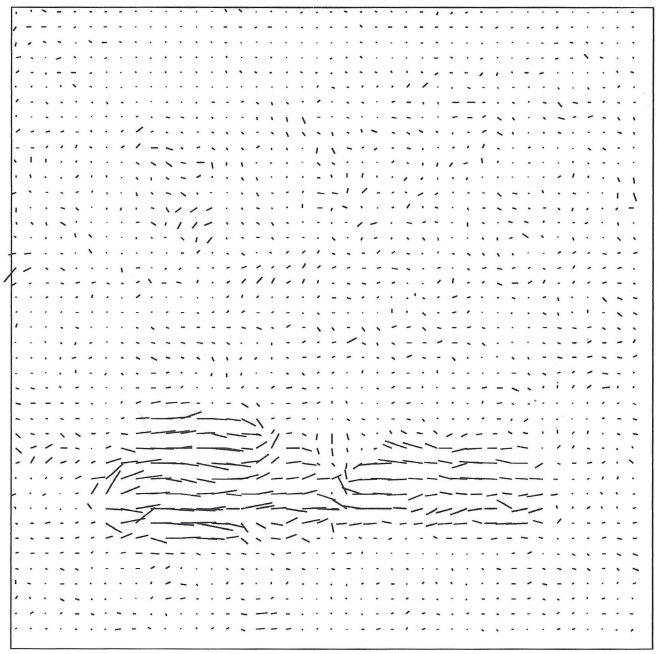

(b) 100

Figure 17. (b) without the penalty constraint ($\alpha = 3$)

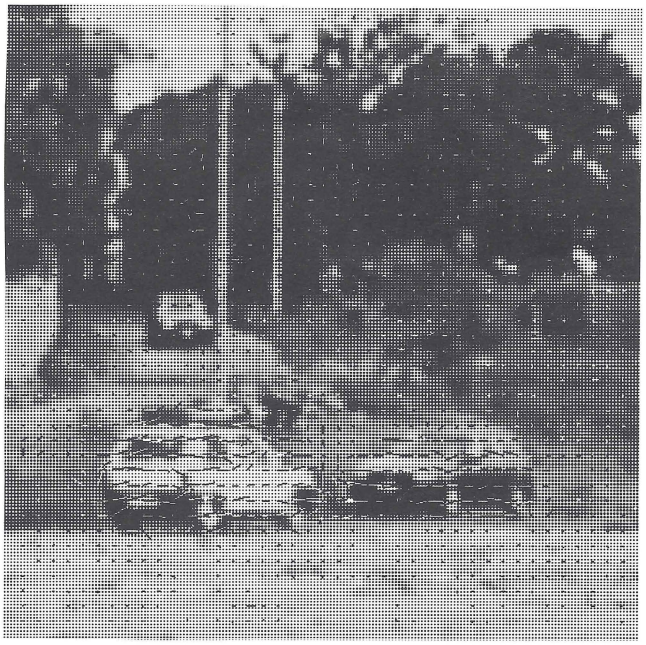

(a) 40

(b) 40

Figure 18. Optical flow fields (40th iteration) superimposed on the 2nd frame of the sequence in Figure 16 obtained using the solutions: (a) with the discontinuity-dependent penalty constraint ($\alpha = 3$, $\beta = 4$, $k = 4$); (b) without the penalty constraint ($\alpha = 3$)

the method proposed estimates, at the first iteration, velocity vectors which are parallel to the image brightness gradient, ∇E in accordance with equation (3). In the absense of the aperture problem, the optical flow vectors, estimated at the first iteration, tend to assume the correct directions with an increasing number of iterations; while in the presence of the aperture problem, the iterative process again tends to regularize the estimated optical flow, but the obtained velocity vectors maintain a direction parallel to the image brightness gradient. This leads to incorrect results with respect to the real motion of the pattern inside the aperture (see Figures 21 and 22). On the other hand, also in this case, the solution proposed maintains the

(a) 20

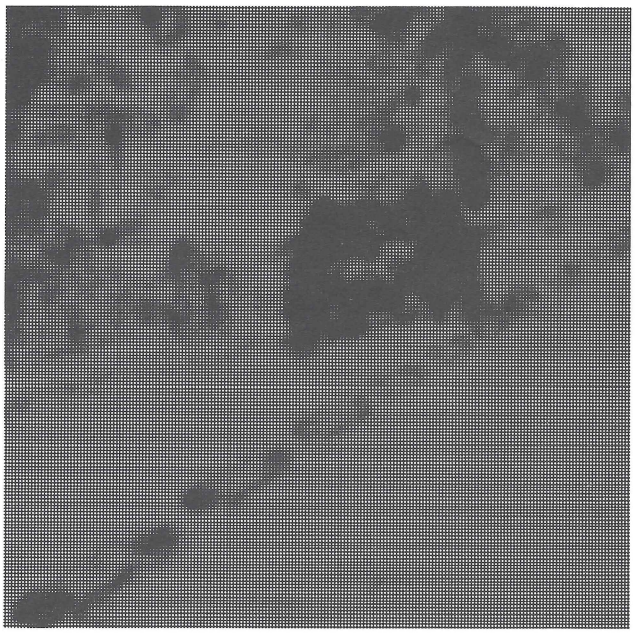

(b) 20

Figure 19. (a) Optical flow field estimated using the solution with the discontinuity-dependent penalty constraint ($\alpha = 3$, $\beta = 1.5$, $k = 3$) (20th iteration), superimposed on the 23rd frame of the test sequence) (b) corresponding map of the control function z, 1×1 pixels of resolution

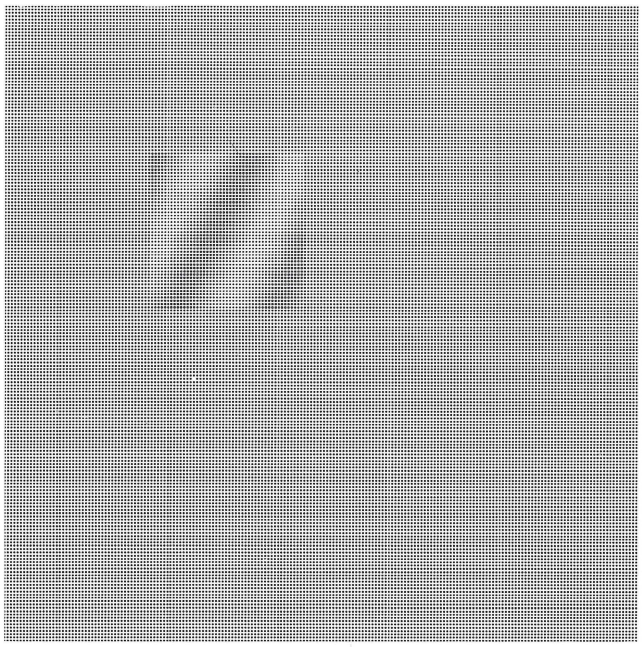

1

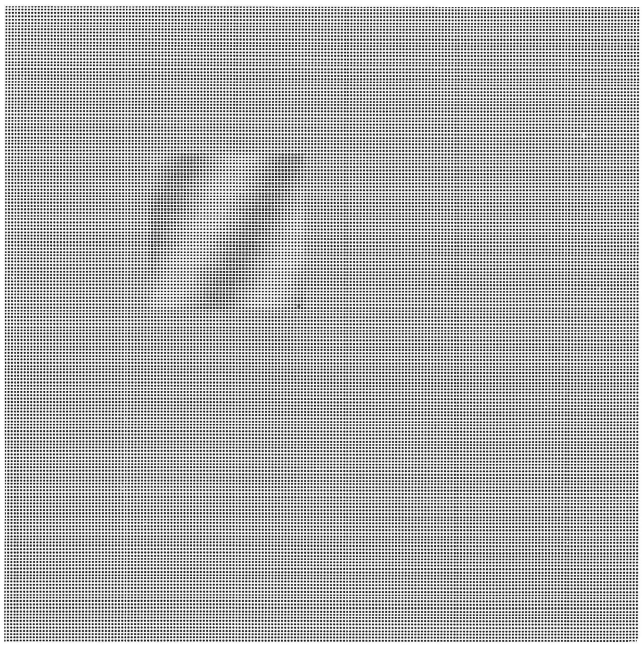

6

Figure 20. Sequence of images where a transversal sinusoidal pattern moving at 180° with respect to the x*-axis is seen through an aperture (1st and 6th frame, 128×128 image resolution)*

profile of the aperture and again avoids all propagation effects.

REGULARIZATION OF OTHERWISE ESTIMATED OPTICAL FLOWS

In many cases, the optical flow fields estimated with multiconstraint-based methods need to be filtered to be profitably used[7,8]. For example, it is better to have smoother solutions in order to use the optical flow for moving object segmentation and object tracking, as well as for estimation of ego-motion. On the other hand, the filtering can destroy important information for both 3D object reconstruction and 3D motion estimation.

In this section, it is shown that the penalty constraint

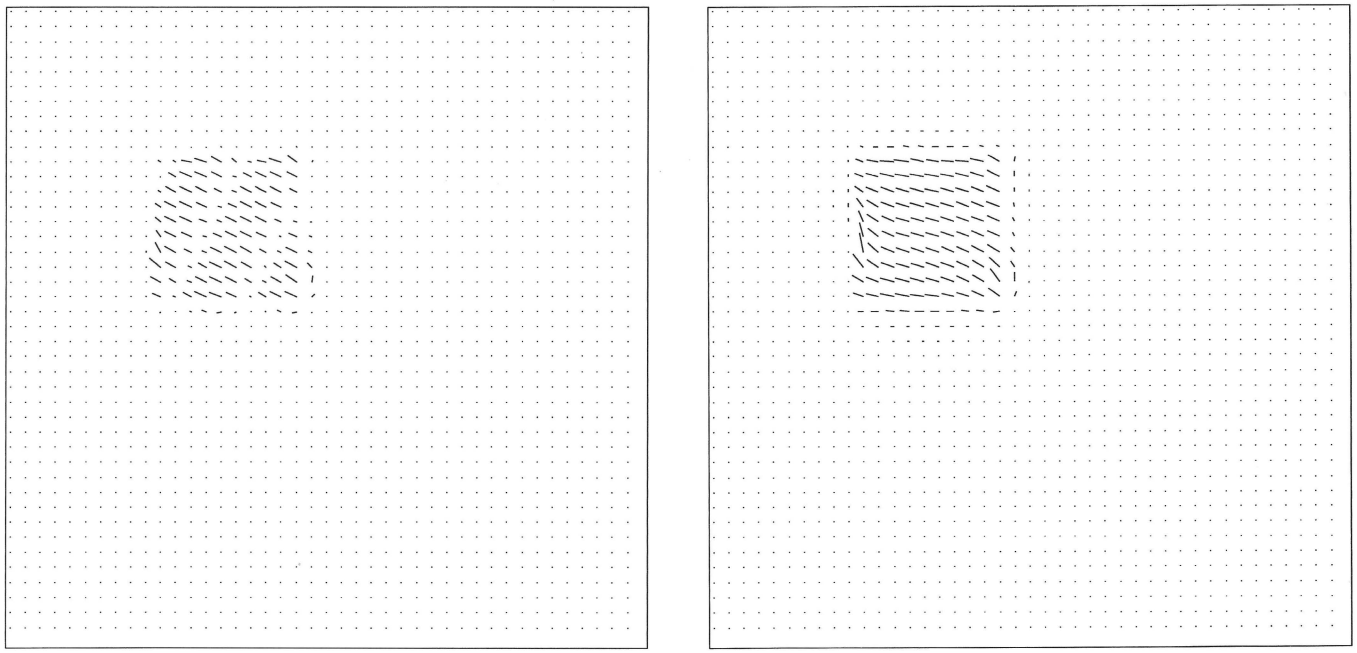

3 99

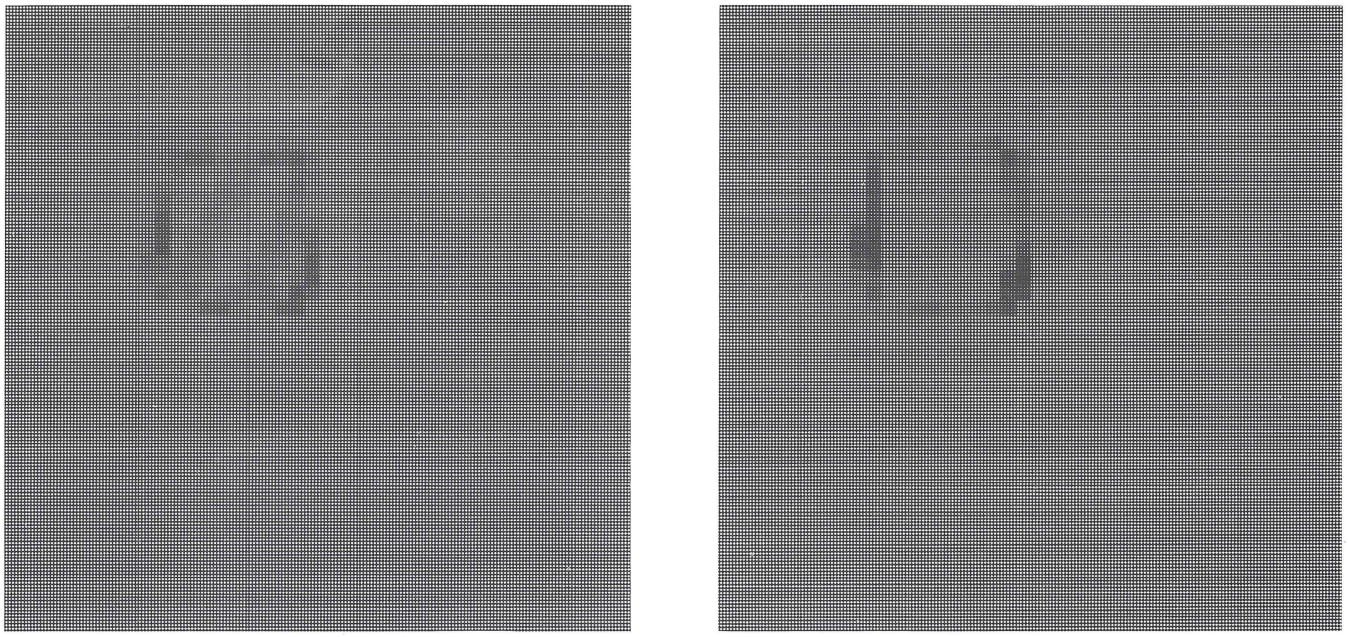

3 99

Figure 21. Optical flow and maps of the control function z *on the 5th frame of the sequence in Figure 20 obtained using the solution with the discontinuity-dependent penalty constraint (iterations: 3, 99), ($\alpha = 3$, $\beta = 1.3$, $k = 5$)*

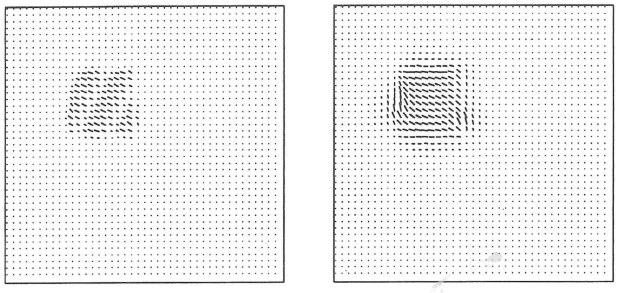

3 99

Figure 22. Optical flow estimation on the 5th frame of the sequence in Figure 20 obtained using the solution without the penalty constraint ($\alpha = 3$, iterations: 3, 99)

can be profitably used to define a method for smoothing noisy optical flow fields estimated by other methods, such as the multiconstraint-based method. This method can be used instead of other techniques such as optical flow filtering (e.g. post-filtering). The goals of this smoothing action are to reduce the discontinuities caused by noise, and to preserve the discontinuities due to the object boundaries with respect to the background and other moving objects. In this way, the problem of object boundary loss, caused by the use of wide Gaussian filters or averaging of the estimated optical flow, are strongly reduced.

The regularization problem is formulated as the minimization of a functional comprised of three terms: the first is the lack of regularity of the estimated optical flow field (u, v) with respect to the smoothed optical flow (U, V); the second is a measure of the smoothness of the final optical flow; and the last is the discontinuity-dependent penalty constraint:

$$F=\int\int\Big[(u-U)^2+(v-V)^2 +\alpha^2 z^2(U_x^2+U_y^2+V_x^2+V_y^2) +\beta^2\Big(\frac{\|\nabla z\|^2}{k}+\frac{k(1-z)^2}{4}\Big)\Big]\,dx\,dy$$

where α^2 is a weighing factor which controls the action of the smoothing factor, and z is the control function. Also in this case, the factors β and k assume the same meaning as discussed earlier in the section on variational convergence for optical flow estimation. The functional is minimized by using the calculus of variation to obtain three linear partial differential equations:

$$\alpha^2 z^2(U_{xx}+U_{yy})+2\alpha^2 z(U_x z_x+U_y z_y)+u-U=0 \quad (8)$$

$$\alpha^2 z^2(V_{xx}+V_{yy})+2\alpha^2 z(V_x z_x+V_y z_y)+v-V=0 \quad (9)$$

$$\frac{\beta^2}{k}(z_{xx}+z_{yy})+\frac{\beta^2 k}{4}(1-z)-\alpha^2 z(U_x^2+U_y^2+V_x^2+V_y^2)=0$$

A discrete version of these equations can be obtained using the finite difference method:

$$4\alpha^2 z_{i,j,t}^2(\bar{U}_{i,j,t}-U_{i,j,t})+2\alpha^2 z_{i,j,t}(U_{xi,j,t}z_{xi,j,t}+U_{yi,j,t}z_{yi,j,t})+u_{i,j,t}-U_{i,j,t}=0 \quad (10)$$

$$4\alpha^2 z_{i,j,t}^2(\bar{V}_{i,j,t}-V_{i,j,t})+2\alpha^2 z_{i,j,t}(V_{xi,j,t}z_{xi,j,t}+V_{yi,j,t}z_{yi,j,t})+v_{i,j,t}-V_{i,j,t}=0 \quad (11)$$

$$4\frac{\beta^2}{k}(\bar{z}_{i,j,t}-z_{i,j,t})+\frac{\beta^2 k}{4}(1-z_{i,j,t})-\alpha^2 z_{i,j,t}(U_{xi,j,t}^2+U_{yi,j,t}^2+V_{xi,j,t}^2+V_{yi,j,t}^2)=0$$

By adopting the method of Jacobi, and by using the average of the control function $\bar{z}_{i,j,t}$ instead of the local value $z_{i,j,t}$, the expressions for $U_{i,j,t}^{n+}$, $V_{i,j,t}^{n+}$ for the

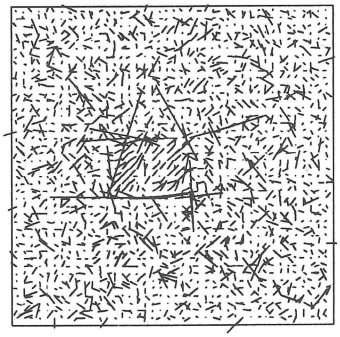

Figure 23. Noisy optical flow field estimated using a multiconstraint-based method on the sequence presented in Figure 2 (5th frame)

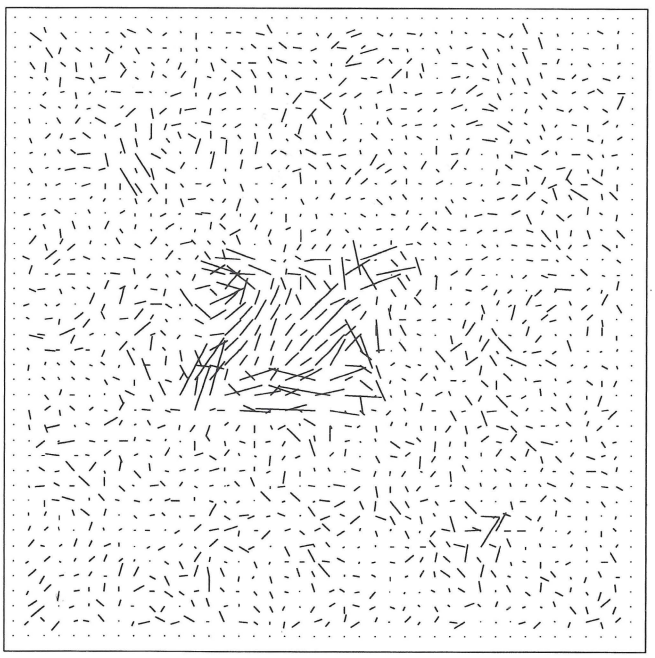

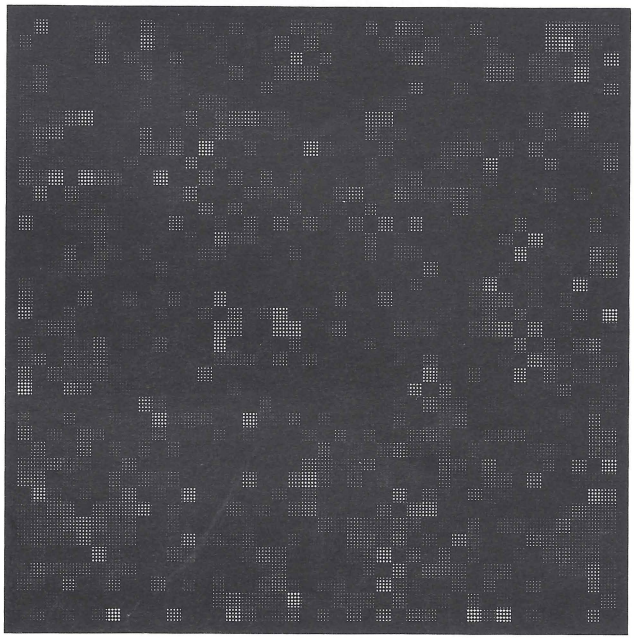

1

Figure 24.

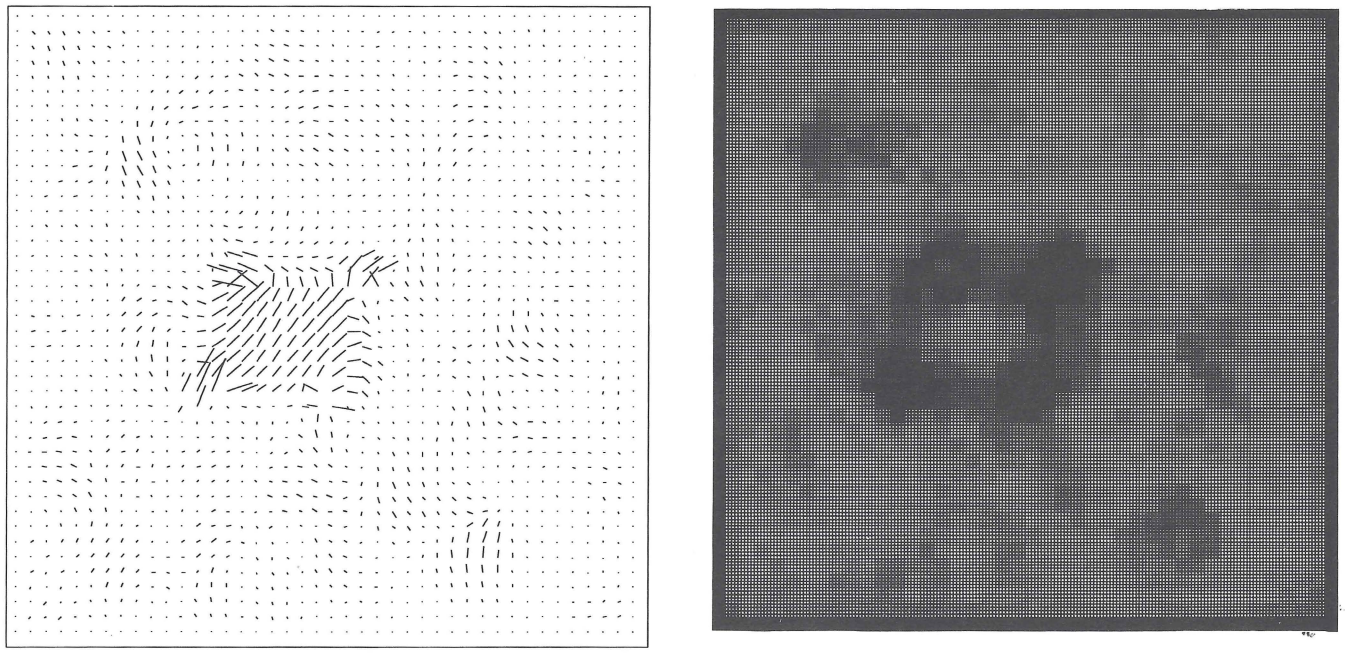

5

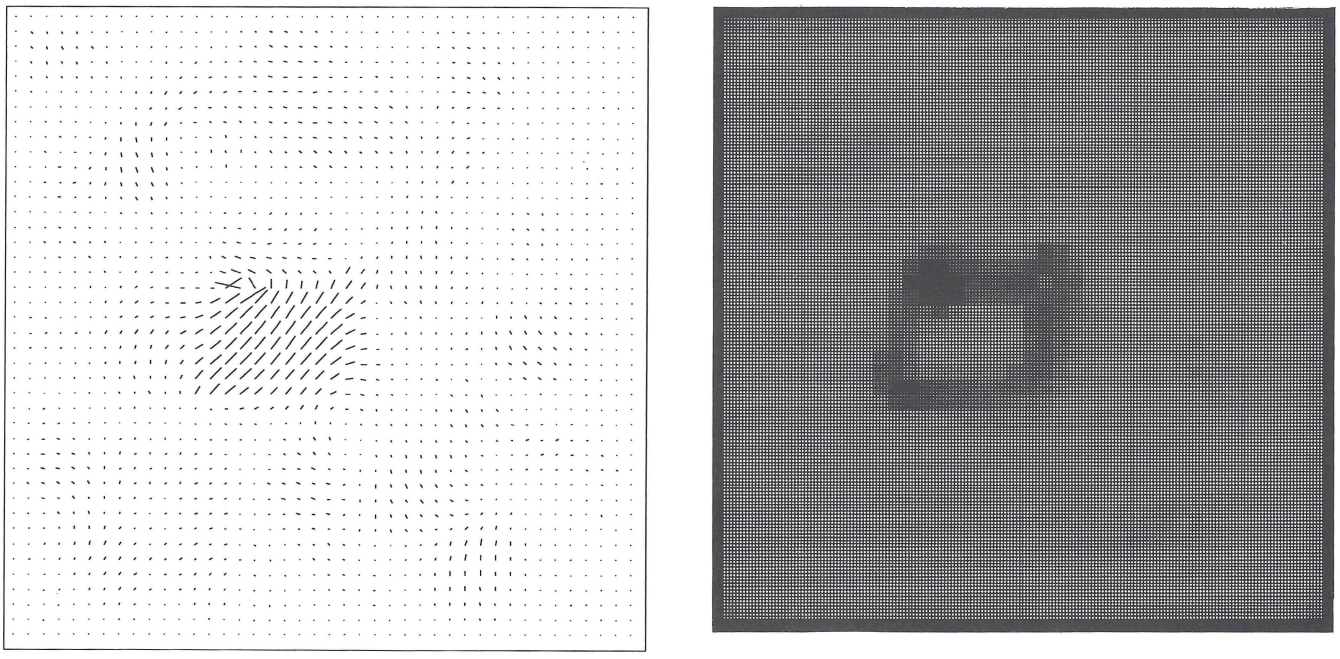

10

Figure 24. Optical flow field and maps of the control function z. 1st, 5th, and 10th iterations of the regularization of noisy optical flow presented in Figure 23 ($\alpha = 3$, $\beta = 1.3$, $k = 5$)

proposed iterative solution becomes:

$$U^{n+1}_{i,j,t} = \frac{u^n_{i,j,t} + 4\alpha^2(\bar{z}^n_{i,j,t})^2 \bar{U}^n_{i,j,t} + 2\alpha^2 \bar{z}^n_{i,j,t}(U^n_{xi,j,t} z^n_{xi,j,t} + U^n_{yi,j,t} z^n_{yi,j,t})}{1 + 4\alpha^2(\bar{z}^n_{i,j,t})^2}$$

$$V^{n+1}_{i,j,t} = \frac{v^n_{i,j,t} + 4\alpha^2(\bar{z}^n_{i,j,t})^2 \bar{V}^n_{i,j,t} + 2\alpha^2 \bar{z}^n_{i,j,t}(V^n_{xi,j,t} z^n_{xi,j,t} + V^n_{yi,j,t} z^n_{yi,j,t})}{1 + 4\alpha^2(\bar{z}^n_{i,j,t})^2}$$

$$X^{n+1}_{i,j,t} = \frac{\bar{z}^n_{i,j,t} 16 + k^2}{k^2 + 4k(\alpha^2/\beta^2)((U^n_{xi,j,t})^2 + (U^n_{yi,j,t})^2 + (V^n_{xi,j,t})^2 + (V^n_{yi,j,t})^2) + 16}$$

where i, j are the point coordinates of the optical flow estimation grid, t is the time, n is the iteration number, and $u^n_{i,j,t} = U^n_{i,j,t}$, $v^n_{i,j,t} = V^n_{i,j,t}$.

These smoothing equations can be used on noisy optical flow fields (such as that in Figure 23) to improve their quality. As can be seen by observing the example

reported in Figure 24, a smoother optical flow field is obtained in a few iterations while maintaining the object boundaries.

CONCLUSIONS

One of the main problems in estimating optical flow is the presence of discontinuities. In the past, many different regularization techniques were adopted in an attempt to solve this problem. The main drawback of these solutions is the presence of propagation effects, which produce a loss of information associated with the discontinuities. On the other hand, this information is very important for detecting the shape of moving objects. In this paper, the theory of variational Γ-convergence has been adopted to obtain a new solution for optical flow estimating which maintains the information related to the discontinuities. It is shown that this solution produces good results in the presence of discontinuities caused by noise, occlusions, and also maintains the moving object profiles. In addition, it has been shown that this theory can also be profitably used to define an iterative process to regularize the optical flow fields estimated by other methods, such as the multiconstraint-based methods, which usually adopt filters that destroy the information associated with discontinuities.

ACKNOWLEDGEMENTS

The author wishes to thank A Del Bimbo and J L C Sanz for their discussions about optical flow estimation techniques in general, and the referees for their useful suggestions for the improvement of this paper.

REFERENCES

1 **Ullman, S** *The Interpretation of Visual Motion,* MIT Press, Cambridge, MA (1979)
2 **Davis, L S, Wu, Z and Sun, H** 'Contour-based motion estimation', *Comput. Vision, Graph. & Image Process.,* Vol 23 (1983) pp 313–326
3 **Duncan, J H and Chou, T** 'Temporal edges: the detection of motion and the computation of optical flow', *Proc. 2nd IEEE Int. Conf. on Comput. Vision,* Tampa, FL (1988)
4 **Fennema, G L and Thompson, W B** 'Velocity determination in scene containing several moving objects', *Comput. Graph. & Image Process.,* Vol 9 (1979) pp 301–315
5 **Horn, B K P and Schunck, B G** 'Determining optical flow', *Artif. Intell.,* Vol 17 (1981) pp 185–203
6 **Nagel, H H** 'Displacement vectors derived from second-order intensity variations in image sequences', *Comput. Vision, Graph. & Image Process.,* Vol 21 (1983) pp 85–117
7 **Haralick, R M and Lee, J S** 'The facet approach to optical flow' in **L S Baumann (ed),** *Proc. Image Understanding Workshop*, Science Applications Arlington, VA (1983)
8 **Tretiak, O and Pastor, L** 'Velocity estimation from image sequences with second order differential operators', *Proc. 7th IEEE Int. Conf. on Patt. Recogn.,* Montreal, Canada (1984) pp 16–19
9 **Verri, A and Poggio, T** 'Motion field and optical flow: Qualitative properties', *IEEE Trans. PAMI,* Vol 11 No 5 (May 1989) pp 490–498
10 **Nagel, N H** 'On a constraint equation for the estimation of displacement rates in image sequences', *IEEE Trans. PAMI.*, Vol 11 No 1 (January 1989) pp 13–30
11 **Nesi, P, Del Bimbo, A and Sanz, J L C** *A unified approach to optical flow constraint analysis,* Technical report, Dipartimento di Sistemi e Informatica, Facoltá di Ingegneria, Universitá di Firenze, DSI-RT 17/92 (1992)
12 **Hadamard, J** *Sur les problems aux derivees patielles et leur signification physique,* Vol 13, Princeton University Bulletin (1902)
13 **Hadamard, J** *Lectures on the Cauchy problem in Linear Partial Differential Equations*, Yale University Press, CT (1923)
14 **Verri, A, Girosi, F and Torre, V** 'Differential techniques for optical flow', *J. Opt. Soc. Am. A,* Vol 7 No 5 (May 1990) pp 912–922
15 **Bertero, M, Poggio, T A and Torre, V** 'Ill-posed problems in early vision', *Proc. IEEE,* Vol 76 No 8 (August 1988) pp 869–889
16 **John, F** 'Countinuous dependence on data for solutions of partial differential equations with a prescribed bound', *Commun. Pure & Appl. Math.,* Vol 13 (1960) pp 551–585
17 **DeGiorgi, E** Γ*-convergenza e G-convergenza,* Technical Report 2, Bollettino Unione Matematica Italiana (1977)
18 **Ambrosio, L and Tortorelli, V M** 'Approximation of functionals depending on jumps by elliptic functionals via Γ-convergence', *Commun. Pure & Appl. Math.,* Vol 43 (1990) pp 999–1036
19 **Poggio, T** 'Early vision: From computational structure to algorithms and parallel hardware', *Comput. Graph. & Image Process.,* Vol 31 (1985) pp 139–155
20 **Poggio, T, Torre, V and Koch, C** 'Computational vision and regularization theory', *Nature*, Vol 317 (26 September 1985) pp 314–319
21 **Torre, V and Poggio, T** 'On edge detection', *IEEE Trans. PAMI,* Vol 8 No 2 (March 1986) pp 147–163
22 **Terzopoulos, D** 'Regularization of inverse visual problems involving discontinuties', *IEEE Trans. PAMI,* Vol 8 No 4 (July 1986) pp 413–424
23 **Terzopoulos, D** 'Image analysis using multigrid relaxation methods', *IEEE Trans. PAMI,* Vol 8 No 2 (March 1985) pp 129–139
24 **Tikhonov, A N and Arsenin, V Y** *Solution of Ill-Posed Problems*, Winston & Sons, DC (1977)
25 **Courant, R and Hilbert, D** *Methods of Mathematical Physic,* Vol 1, Interscience Publishers, NY (1955)
26 **Schunck, B G** 'Image flow segmentation and estimation by consrtaints line and clustering', *IEEE Trans. PAMI,* Vol 11 No 10 (October 1989) pp 1010–1027
27 **Yachida, M** 'Determining velocity maps by spatio-temporal neighbourhoods from image sequences', *Comput. Vision. Graph. & Image Process.,* Vol 21 (1983) pp 262–279
28 **Nagel, H H and Enkelmann, W** 'An investigation of smoothness constraints for the estimation of

displacement vector fields from image sequences', *IEEE Trans. PAMI.,* Vol 8 No 5 (September 1986) pp 565–593

29 **Konrad, J and Dubois, E** 'Multigrid bayesian estimation of the image motion fields using stochastic relaxation', *Proc. 2nd IEEE Int. Conf. on Comput. Vision,* Tampa, FL (1988) pp 354–362

30 **Schnörr, C** 'Computation of discontinuous optical flow by domain decomposition and shape optimization', *Int. J. Comput. Vision,* Vol 8 No 2 (1992) pp 153–165

31 **Hildreth, E C** 'Computations underlying the measurement of visual motion', *Artif. Intell.,* Vol 23 (1984) pp 309–354

32 **Hildreth, E C** 'Computing the velocity field along contours', in **Badler, N I and Tsotsos, J K (eds),** *Motion: Representation and Perception,* Elsevier, Netherlands (1986)

33 **Woodham, R J** 'Multiple light source optical flow', *Proc. 3rd IEEE Int. Conf. on Comput. Vision,* Osaka, Japan (4–7 December 1990) pp 42–46

34 **Markandey, V and Flichbaugh, B E** 'Multispectral constraints for optical flow computation', *Proc. 3rd IEEE Int. Conf. on Comput. Vision,* Osaka, Japan (4–7 December 1990) pp 38–41

35 **Mitiche, A, Wang, Y F and Aggarwal, J K** 'Experiments in computing optical flow with the gradient-based multiconstraint method', *Patt. Recogn.,* Vol 20 No 2 (1987) pp 173–179

36 **Campani, M and Verri, A** 'Computing optical flow from an overconstrained system of linear algebraic equation', *Proc. 3rd IEEE Int. Conf. on Comput. Vision,* Osaka, Japan (4–7 December 1990) pp 22–26

37 **Nesi, P, Del Bimbo, A and Sanz, J L C** 'Multiconstraints-based optical flow estimation and segmentation', *Int. Workshop on Comput. Architecture for Machine Perception,* Paris, France (December 1991) pp 419–426

38 **Blake, A and Zisserman, A** *Visual Reconstruction,* MIT Press, Cambridge, MA (1987)

39 **March, R** 'Visual reconstruction with discontinuities using variational methods', *Image & Vision Comput.,* Vol 10 No 1 (January 1992) pp 30–38

40 **Mumford, D and Shah, J** 'Optimal approximations by piecewise smooth functions and associated variational problems', *Commun. Pure & Appl. Math.,* Vol 42 No 5 (May 1989) pp 577–685

41 **Modica, L and Montorla, S** *Il limite nella Γ-convergenza di una famiglia di funzionali ellittici,* Technical Report 3, Bollettino Unione Matematica Italiana (1977)

42 **Vemuri, V and Karplus, W J** *Digital Computer Treatment of Partial Differential Equations,* Prentice-Hall, NJ (1981)

43 **Nagel, H H and Enkelmann, W** 'Towards the estimation of displacement vector fields by 'oriented smoothness' constaints', *Proc. 7th IEEE Int. Conf. on Patt. Recogn.*, Montreal, Canada (1984) pp 6–8

44 **Nagel, H H** 'On the estimation of dense displacement maps from image sequences', *ACM Motion Workshop,* Toronto, Canada (1983) pp 59–65